General Disclaimer

One or more of the Following Statements may affect this Document

- This document has been reproduced from the best copy furnished by the organizational source. It is being released in the interest of making available as much information as possible.

- This document may contain data, which exceeds the sheet parameters. It was furnished in this condition by the organizational source and is the best copy available.

- This document may contain tone-on-tone or color graphs, charts and/or pictures, which have been reproduced in black and white.

- This document is paginated as submitted by the original source.

- Portions of this document are not fully legible due to the historical nature of some of the material. However, it is the best reproduction available from the original submission.

(NASA-CR-174054) THE STUDY OF MICROSTRIP ANTENNA ARRAYS AND RELATED PROBLEMS Semiannual Report, 22 May - 21 Nov. 1984 (Illinois Univ., Urbana-Champaign.) 42 p HC A03/MF A01 CSCL 20N G3/32

N85-11265

Unclas 24390

THE STUDY OF MICROSTRIP ANTENNA ARRAYS AND RELATED PROBLEMS

Semiannual Report

(22 May 1984 to 21 November 1984)

for

NASA NAG 3-418

National Aeronautics and Space Administration
Lewis Research Center
21000 Brookpark Road
Cleveland, OH 44135

NASA Technical Officer - R. Q. Lee

Prepared by

Y. T. Lo
Electromagnetics Laboratory
Department of Electrical Engineering
University of Illinois at Urbana-Champaign
1406 W. Green St.
Urbana, IL 61801

Technical Work

During this period efforts have been expended for the following tasks:

(1) Microstrip Antenna Module

Because of the physical layout of the array elements and the proximity of the microstrip feed network, the input impedance and radiation pattern values are dependent upon the effects of mutual coupling, feedline discontinuities (e.g., curves, T-junctions, and corners), and feed point location. Consequently, in a first attempt to assess the extent of these dependences, a number of single patch and module structures have been constructed and measured at an operating frequency of approximately 4.0 GHz. These empirical results have then been compared to those theoretically predicted by the cavity model of thin microstrip antennas (Lo, Richards). In doing so, of course, each element has been modelled as an independent radiating patch and each microstrip feedline as an independent, quasi-TEM transmission line (Hammerstad). The effects of the feedline discontinuities have been approximated by lumped L-C circuit models originally developed by Oliner and Milnes.

Two constructed modules are shown in Figure 1 where two key distinguishing features of the structures namely, the individual element feed points and the feed transmission lines, are recognizable. The differences between the two are the direct consequences of the field distribution present within the array elements when the antenna is excited at a frequency near the (0,1) resonance mode frequency of the

patches- a condition in which side "a" of each patch exhibits no electric field variation while that of side "b" exhibits one half cycle of sinusoidal variation. Use has been made of this fact in the structure depicted in Figure 1.a where it is seen that relocation of the feed point along the "b" edge results in patch input impedance variation in much the same manner that impedance varies along a uniform transmission line not terminated in its own characteristic impedance. The second difference likewise stems from the relocation of the feed point, but is visible in the simplification of the microsrtip feed network which is necessarily required to be symmetrical in phase length if the antenna module is to produce a single, broadside, mainbeam. Because of these motivations, versions of both the commonly used module/feed network (Figure 1.b) and the modified structure (Figure 1.a) have been implemented and tested.

To examine the utility of the cavity model when used in conjunction with substrates thicker (~0.025 free space wavelengths) than that used previously (Lo, Richards), numerous single patch devices were constructed on substrates of differing relative dielectric constants and fed by narrow microstrip (Zo= 100 to 150 Ohms) or coaxial cable. The resulting input impedances were then measured and compared to theoretically obtained values. One such case is seen in Figure 2 where, as can be seen in the plot, the agreement between theory and experiment is very good.

In a similar manner, the input impedances of the subarray modules were then measured and computed. The computations were identical to those of the single patch case, except of course for the evaluation of

the microstrip T-junctions and corners and for the transformation of the impedances throughout the feed network. The results for the modules of Figure 1.a and 1.b are shown in Figure 3.a and 3.b, respectively. In Figure 3.a, one sees some agreement between theory and experiment but, in Figure 3.b, severe distortion of the impedance locus is apparent, perhaps due to the increased number of feed line corners and T-junctions and the increased interaction of the feed lines with themselves as well as the array elements.

For the analysis of E plane radiation patterns, theoretical plots were obtained by computing the pattern of a single patch having the same dimensions as those of the array elements and by performing pattern multiplication. The absence of mutual coupling was assumed and the corresponding array factor for two dimensional arrays employed. In the case of the common structure, the theoretically computed beamwidth (Figure 4) is consistently narrower than that obtained experimentally, but correctly accounts for the absence of side lobes and a significant cross polarization component. Contrarily, for the modified structure, the theoretical plot is consistently broader than the experimental and predicts a higher broadside cross polarization magnitude than that which was actually measured.

Also, it has been determined that previously written software to be used in the analysis of rectangular microstrip antennas contains minor programming errors. Modifications to the program (A Fortran Program For Rectangular Microstrip Antennas, University of Illinois at Urbana Champaign, RADC-TR-82-78, Interim Report, April 1982) are given in the appendix.

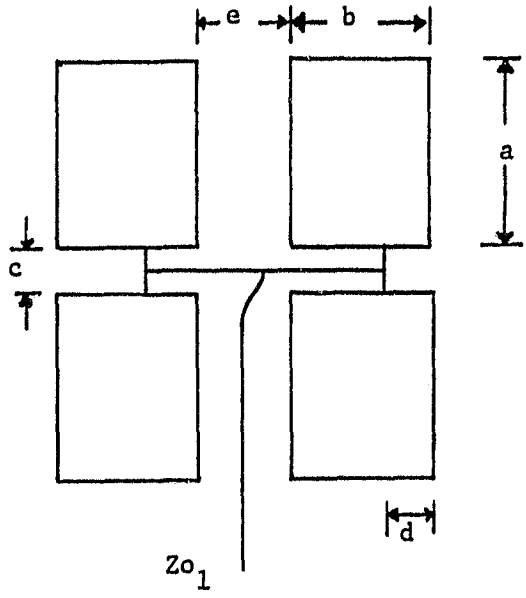

Figure 1.a

a = 3.0 cm

b = 2.45 cm

c = 0.75 cm

d = 0.80 cm

e = 1.3 cm

f = 1.5 cm

Zo_1 = 104 Ohms

Zo_2 = 125 Ohms

ϵ_r = 2.48

$f_{op.}$ = 3.88 GHz

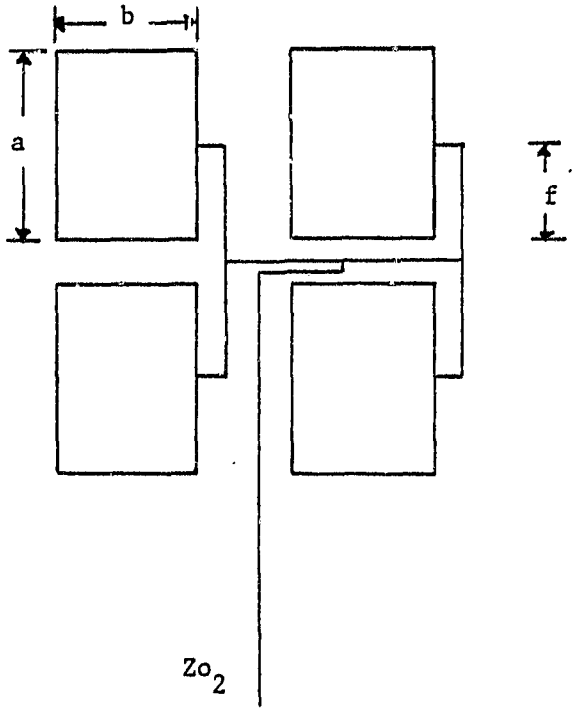

Figure 1.b

Single Patch
a = 4.0 cm
b = 2.43 cm
x = 2.0 cm
y = 0.5 cm
ϵ_r = 2.62
Freq. in GHz

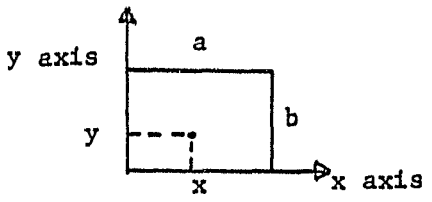

Theoretical = dotted
Experimental = continuous

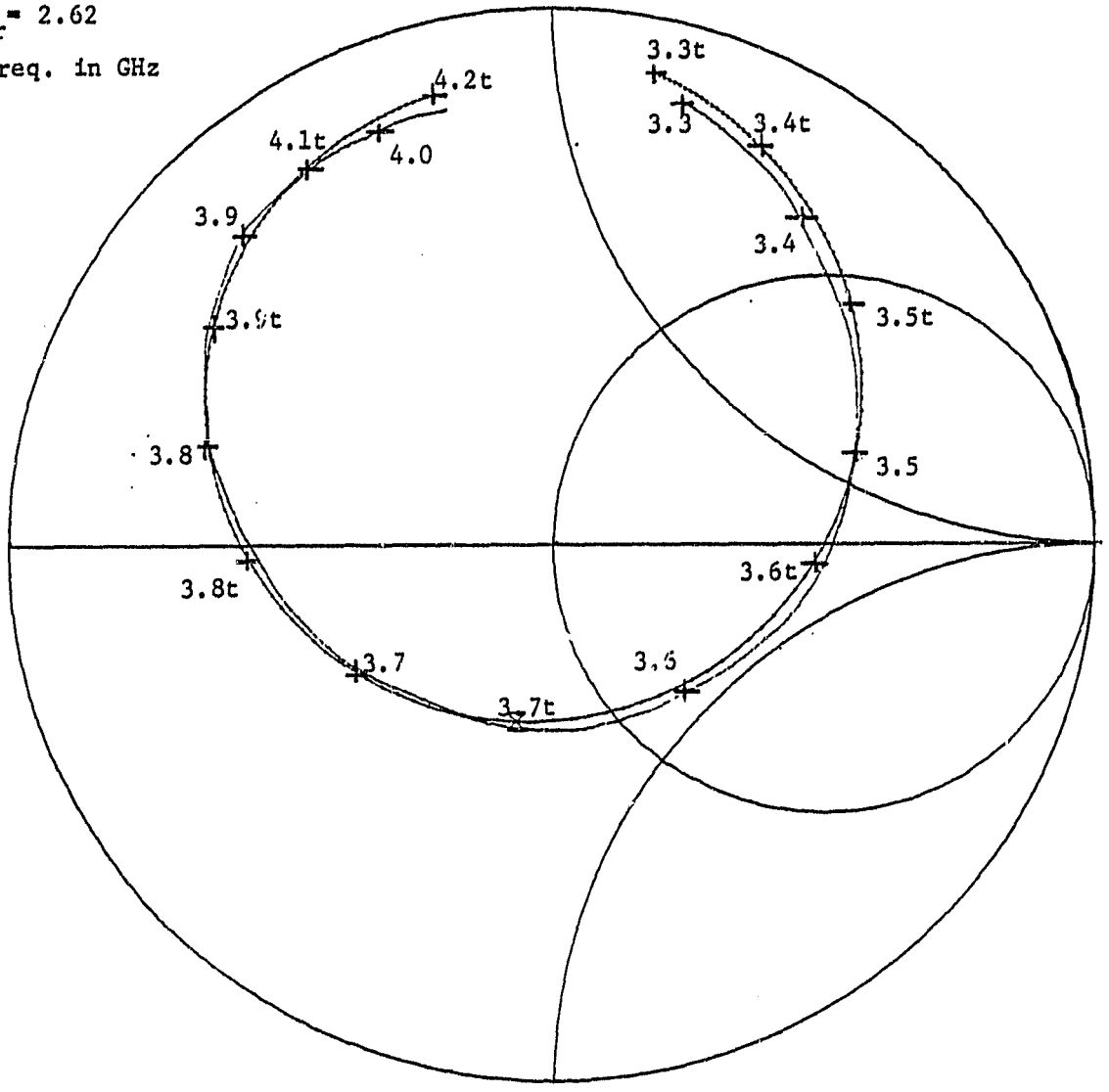

Figure 2

Modified Array Module Input Impedance
a = 3.0 cm
b = 2.45 cm
ϵ_r = 2.48
Zo_1 = 104 Ohms
d = 0.8 cm
Freq. in GHz

Theoretical = dotted
Experimental = continuous

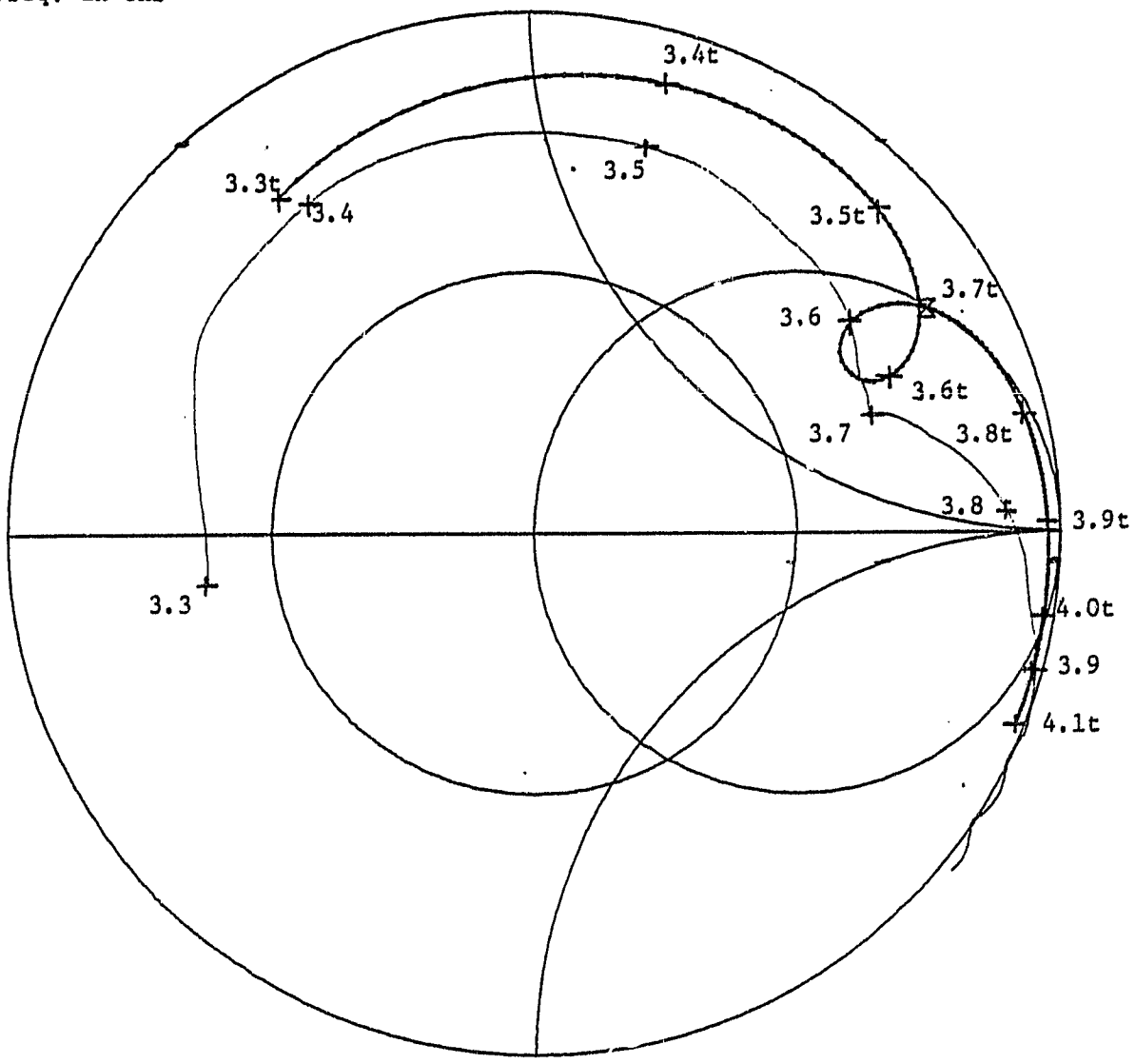

Figure 3.a

Common Array Module Input Impedance
a = 3.0 cm
b = 2.45 cm
ϵ_r = 2.48
Zo_2 = 125 Ohms
f = 1.5 cm
Freq. in GHz

Theoretical = dotted
Experimental = continuous

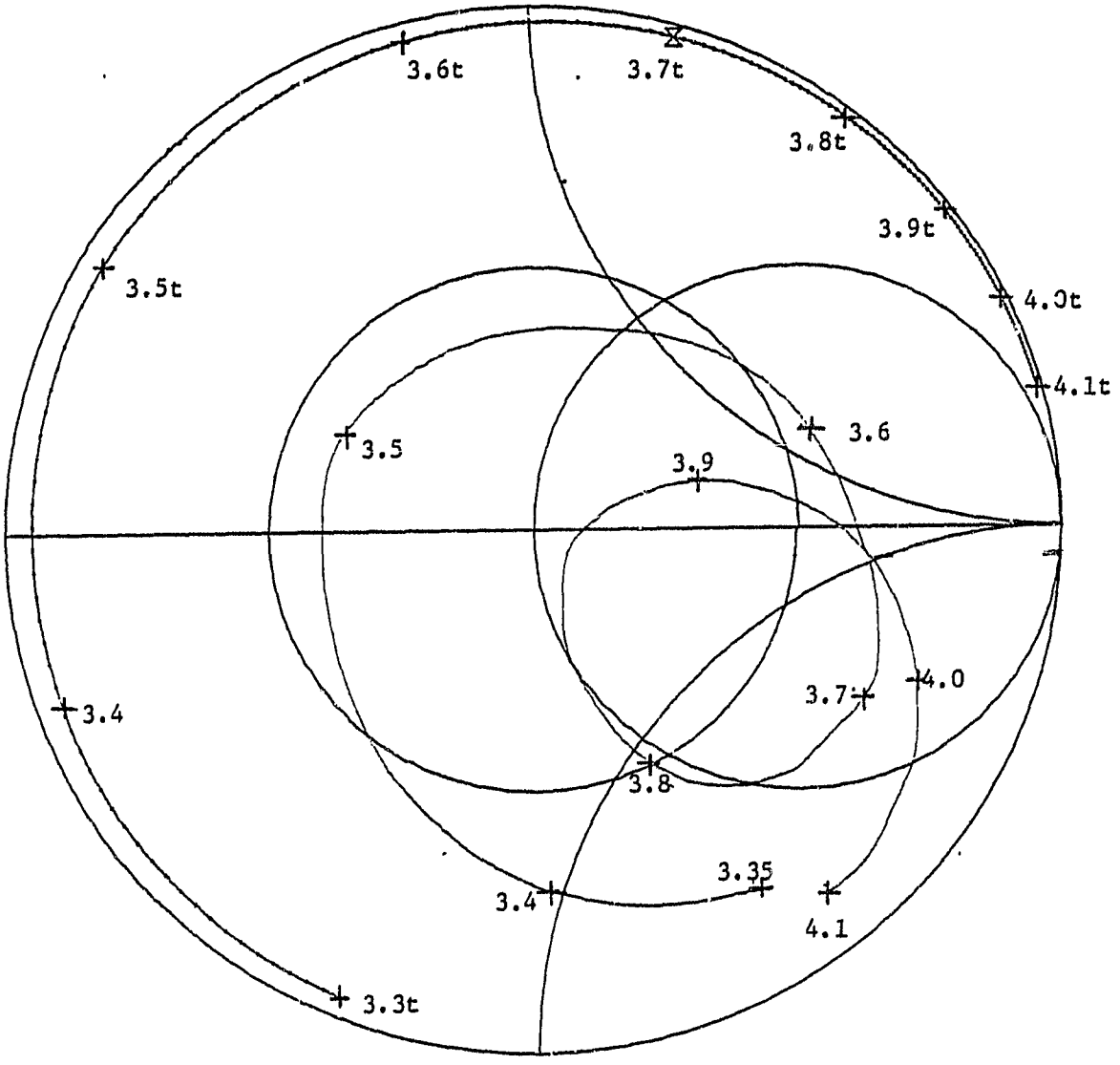

Figure 3.b

Modified Structure
Theoretical = solid
Experimental = dotted
E-Plane Pattern

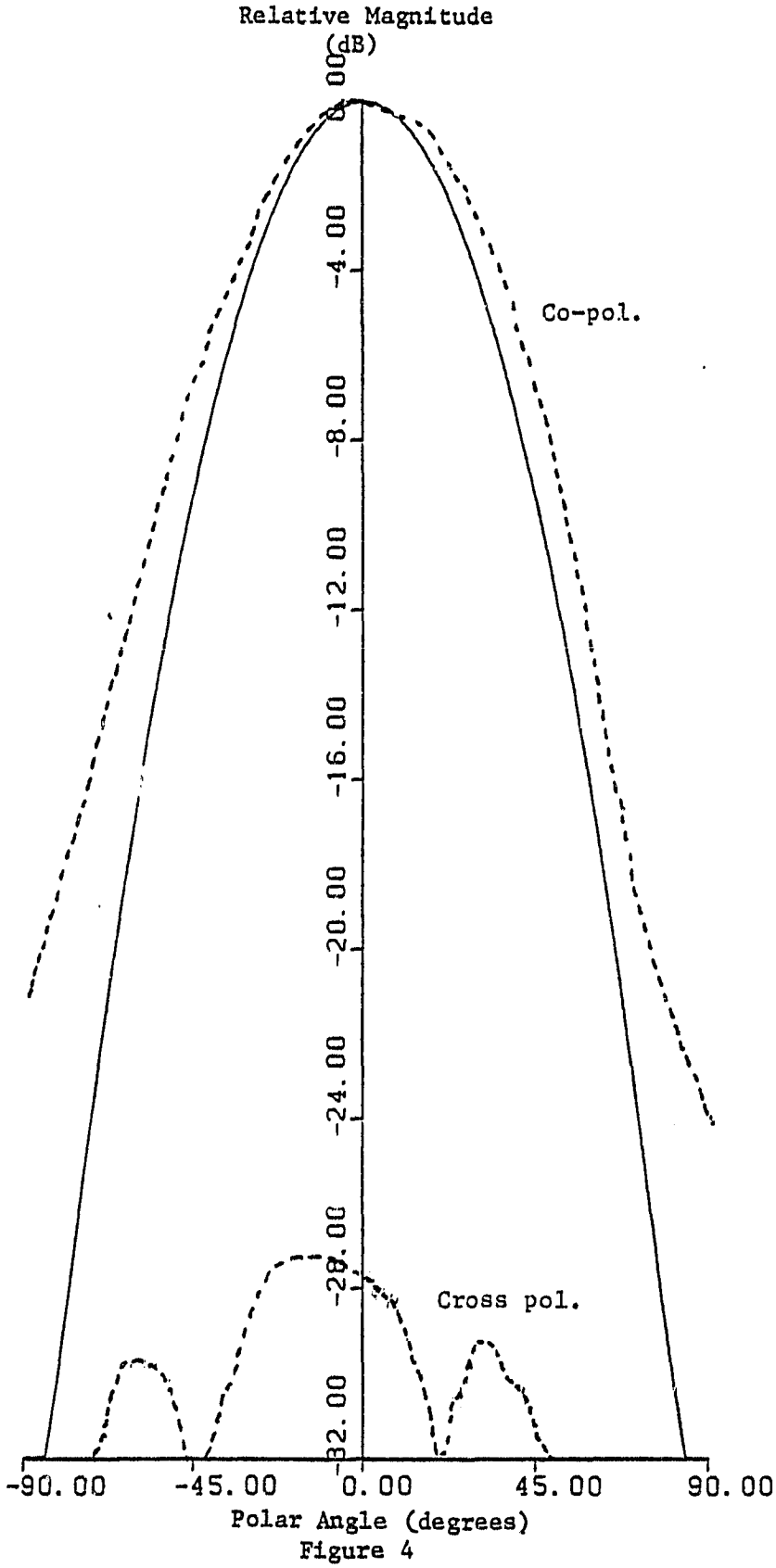

Figure 4

During the next period it is intended that a completed matching network/array structure having an impedance and pattern bandwidth of at least two percent be obtained.

(2) Dual Frequency Antennas

By using both slots and shorting pins, the ratio of two operating frrequency bands can be varied over a wide range, thus making the design much more useful. A paper was published in the IEEE Transactions on Antennas and Propagation September, 1984. A copy of this paper is attached in the appendix section. At the moment, we consider this project completed unless an idea or a new application is evolved.

(3) CP Microstrip Antennas

A thin microstrip antenna can be designed to produce CP waves, in fact waves of any polarization, without using phasing and power-dividing networks. However, both theory and experiment show that the CP bandwidth (for 3 dB axial ratio) is very narrow, namely (35/Q)%. For substrate of a few thousandths of a wavelength thick, Q is on the order of 100, thus resulting a CP bandwidth only a small fraction of one percent. Suggestion has been made that a differnt design for a nearly square patch with feed located not along the diagonal line could give a wider band. This investigation shows that this speculation is unfounded. The only effective method for broadbanding is to increase the substrate thickness.

Unfortunately, up to the present there is no theory for thick CP microstrip antannas available. On the other hand, we have no knowledge of the upper limit in the thickness below which the theory we developed previously is applicable. In this period we investigated a number of CP microstrip antennas with various thicknesses, all designed on the basis of our microstrip antenna theory. To our surprise, the theory appears to be still useful even for thickness as much as 0.084x(dielectric wavelength). For this case the CP bandwidth is respectable 3.3%. A paper was presented at the 1984 Antenna Applications Symposium. A copy is also attached in the appendix section.

(4) Feed Study

In recent years, several groups of workers (University of Massachusetts, UCLA, MIT, University of Illinois) have attempted to formulate and to solve the problem of microstrip antennas of any thickness. Despite some progress, all failed to take the actual feed structure into consideration. We believe the feed structure plays an important role in the input impedance. During this period considerable effort has been made to tackle this problem. We find, unexpectedly, that the problem is very complex and difficult to solve numerically even for the relatively simple model which consists of an off-set coaxial feed to a disk patch. First it requires the solutions of eigenvalues (resonant frequencies) of an infinitely large matrix. When the feed cable is near the edge, the solution becomes unstable. Second, we also need to find the modal fields and third, to match the fields to that of the fixed cable. We intend to continue this investigation.

Personal

During this period the following people have contributed to the work above:

Y. T. Lo, M. Oberhart, B. Engst, B. F. Wang (without pay) and M. Davidowitz.

Travel

Y. T. Lo and B. F. Wang attended and presented their work at the IEEE AP-S International Synposium June 25-29, 1984, at Boston. Y. T. Lo, M. Oberhart, B. Engst, and B. F. Wang attended and presented papers at the 1984 Antenna Applications Synposium at the Allerton Park, Il. September 1984.

REFERENCES

Y. T. Lo, W. F. Richards, "Theory and Experiment on Microstrip Antennas," IEEE Trans. Ant. and Propagat., Vol. AP-27, pp 137-145, March 1979.

Hammerstad, "Equations for Microstrip Circuit Design," Proc. European Microwave Conference, Sept 1975.

H. M. Altschuler, A. A. Oliner, "Discontinuities in the Center Conductor of Symmetric Strip Transmission Lines," IEEE Microwave Theory and Techniques, MTT-8, May 1960.

A. G. Milnes, W. H. Leighton, "Junction Reactance and Dimensional Tolerance Effects on X-Band 3-dB Directional Couplers," IEEE Microwave Theory and Techniques, MTT-19, pp 818-824, Oct 1971.

R. W. Vogel, "Effect of T-Junction Discontinuity on the Design of 3-dB Branchline and Rat-Race Couplers," IEEE Microwave Theory and Techniques, MTT-21, March 1973.

Because of the form of the "y" component of the vector potential, (pp 4, A Fortran Program For Rectangular Microstrip Antennas, University of Illinois at Urbana Champaign, RADC-TR-82-78, Interim Report, April 1982) discontinous pattern plots obtained via subroutine VPAT may result for those values of theta and phi which make the denominator small. The effect is such that the value will never become infinite if the loss tangent is non-zero, but a sizable discontinuity will nevertheless exist for practical values of loss tangent. The following modification has been derived for the special case of a single patch which is fed by microstrip on the "x" side (y=0.0). It enables continous pattern calculation for the cuts phi=0.0, pi/2.0 . A generalized modification for arbitrary cuts and feed points is being examined, but if the patch is edge fed it may, of course, be rotated such that y=0.0.

In subroutine VPAT delete lines:

```
3       YT=-BOA*F*(PMBSPB*EKYSS+CMPLX(0.,KBSS)*XF)/D2
        FACTOR=COS(M*PXOA)*J0(M*PDO2A)/(PMBSPB)
```

Then define "UK" in the complex declaration statement and insert:

```
3       IF((CABS(D2).LE.0.0075).AND.(PHI.EQ.PI/2.0)
       *.AND. Y.EQ.0.0) GO TO 5
        YT=-BOA*F*(PMBSPB*EKYSS+CMPLX(0.,KBSS)*XF)/D2
        GO TO 6
        UK=CMPLX(0.0,1.0)
5       YT=-BOA*F*(CSIN(PMB)/(PMB*2.0)+0.5*(CCOS(PMB)+UK*CSIN(PMB)))
6       FACTOR=COS(M*PXOA)*J0(M*PDO2A)/(PMBSPB)
```

These seven lines are to be inserted in the program specifically at the location of the deleted lines.

Microstrip Antennas for Dual-Frequency Operation

BAO F. WANG AND YUEN T. LO, FELLOW, IEEE

Abstract—**Single element microstrip antennas for dual-frequency operation have been investigated. By placing shorting pins at appropriate locations in the patch, the ratio of two-band frequencies can be varied from 3 to 1.8. In many applications a smaller ratio is desired, and this can be achieved by introducing slots in the patch. In so doing, the ratio can be reduced to less than 1.3. For this type of antenna, a hybrid multiport theory is developed and theoretical results are found to be in excellent agreement with the measured.**

I. INTRODUCTION

ONE OF THE outstanding features of a thin microstrip antenna is its compactness in structure. Unfortunately it is notoriously narrow-banded unless some degree of compactness can be sacrificed by using a thick substrate. In many applications, it is not operation in a continuous wide-band, but, operation in two or more discrete bands that is required. In this case a thin patch capable of operating in multiple bands is highly desirable, particularly for large array application where considerable saving in space, weight, material and cost can be achieved. For that goal, a few attempts have been made [1], [2], by using two or more patch atennas stacked on top of each other, or placed side by side, or using a complex matching network which takes as much space and weight, if not more, as the element itself. Obviously in all those designs, the advantage of compact structure is sacrificed.

From the cavity-model theory, a single patch antenna can easily be made to resonate at many frequencies associated with various modes. But for most applications, all bands are required to have the same polarization, radiation pattern, and input impedance characteristics. It is also desirable to have a single input port and an arbitrary separation of the frequency bands. All of these impose severe constraints on the use of the modes. In this paper we shall describe some methods which can practically achieve all these goals.

An annular patch can have predominantly broadside radiation when excited for the (1, 1), (1, 2) and even the (1, 3) mode. Unlike a circular disk, the frequencies for those modes can be adjusted by choosing the inner and outer radius dimensions. All the aforestated properties can be obtained except that the variation of the two-frequency band ratio is somewhat limited [3].

By making use of the difference in the field distributions for various modes, it is possible to practically tune the operating frequencies associated with those modes independent of each other. One method is to place a series of shorting pins at the nodal lines of, for example, the (0, 3) modal electrical field of a rectangular patch [3]. These pins will have practically no effect on the (0, 3) modal field structure but can have a strong effect on the (0, 1) field and thus raise the (0, 1) modal frequency.

Manuscript received January 9, 1984; revised April 26, 1984. This work was supported in part by RADC/EEAA, Hanscom AFB, MA, and NASA Lewis Research Center, Cleveland, OH.

B. F. Wang is with the Electromagnetics Laboratory, University of Illinois, Urbana, IL 61801, on leave from Beijing Aeronautics and Astronautics Institute, China.

Y. T. Lo is with the Electromagnetics Laboratory, University of Illinois, Urbana, IL 61801.

0018-926X/84/0900-0938$01.00

Therefore the low band frequency can be tuned independently. However, the ratio of the two operating frequencies, F_H/F_L, can be varied only from three to two approximately. On the other hand, if slots are cut in the patch where the magnetic field of the (0, 3) mode is maximum, they can have a strong effect on the (0, 3) modal field but little on the (0, 1) modal field. Thus the operating frequency for the (0, 3) mode can be lowered. By using both slots and pins, the two operating bands can be varied over a wide range. In this paper an analytic theory is developed for this type of antenna and then verified by experiment.

II. A MICROSTRIP ANTENNA EXCITED BY A MAGNETIC CURRENT K

First consider a microstrip antenna excited by a magnetic current K in the slot centered at (x', y') as shown in Fig. 1. Following the cavity model theory [4], the antenna can be considered as a cavity bounded by magnetic walls along its perimeter and electric walls at $z = 0$ and t. Since the substrate thickness t is typically a few hundredths of a wavelength, we can assume that the field excited by the magnetic current

$$\mathbf{K} = \hat{x}[U(x - x' + d_{eff}/2) - U(x - x' - d_{eff}/2)]\,\delta(y - y')\delta(z - t)$$

in the slot is approximately the same as that excited by

$$\mathbf{K} = \hat{x}[U(x - x' + d_{eff}/2) - U(x - x' - d_{eff}/2)]\,\delta(y - y')[U(z) - U(z - t)]/t$$

where d_{eff} is the effective length of the magnetic current strip of one V/M, and $U(\cdot)$ is the unit step function. The field in the cavity due to K can then be found by modal-matching as given below.

In region I $(y' \leq y \leq b)$

$$E_{z1} = \frac{d_{eff}}{at} \sum_{m=0}^{\infty} \frac{\sin(\beta_m y')\cos(m\pi x'/a)}{\sin(\beta_m b)} \cdot j_0\left(\frac{m\pi d_{eff}}{2a}\right) \cos(m\pi x/a)\cos[\beta_m(b - y)],$$

$$H_{x1} = \frac{jd_{eff}}{at\omega\mu_0} \sum_{m=0}^{\infty} \frac{\beta_m \sin(\beta_m y')\cos(m\pi x'/a)}{\sin(\beta_m b)} \cdot j_0\left(\frac{m\pi d_{eff}}{2a}\right) \cos(m\pi x/a)\sin[\beta_m(b - y)],$$

$$H_{y1} = \frac{j\pi d_{eff}}{a^2 t\omega\mu_0} \sum_{m=0}^{\infty} \frac{m \sin(\beta_m y')\cos(m\pi x'/a)}{\sin(\beta_m b)} \cdot j_0\left(\frac{m\pi d_{eff}}{2a}\right) \sin(m\pi x/a)\cos[\beta_m(b - y)]. \quad (1)$$

In region II $(0 \leq y \leq y')$

$$E_{z2} = \frac{-d_{eff}}{at} \sum_{m=0}^{\infty} \frac{\sin[\beta_m(b - y')]\cos(m\pi x'/a)}{\sin(\beta_m b)} \cdot j_0\left(\frac{m\pi d_{eff}}{2a}\right) \cos(m\pi x/a)\cos(\beta_m y),$$

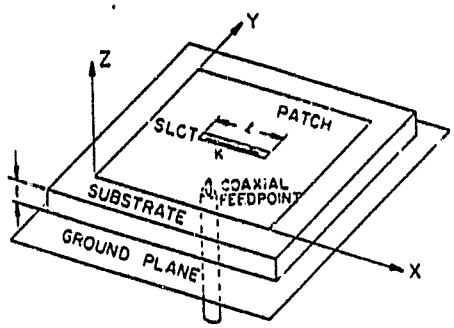

Fig. 1. Geometry of a rectangular microstrip antenna with idealized feeds.

$$H_{x2} = \frac{jd_{eff}}{at\omega\mu_0} \sum_{m=0}^{\infty} \frac{m \sin[\beta_m(b - y')]\cos(m\pi x'/a)}{\sin(\beta_m b)} \cdot j_0\left(\frac{m\pi d_{eff}}{2a}\right) \cos(m\pi x/a)\sin(\beta_m y),$$

$$H_{y2} = \frac{-j\pi d_{eff}}{a^2 t\omega\mu_0} \sum_{m=0}^{\infty} \frac{m \sin[\beta_m(b - y')]\cos(m\pi x'/a)}{\sin(\beta_m b)} \cdot j_0\left(\frac{m\pi d_{eff}}{2a}\right) \sin(m\pi x/a)\cos(\beta_m y), \quad (2)$$

where $\beta_m^2 = k^2 - (m\pi/a)^2$, $k^2 = k_0^2\epsilon_r(1 - j\delta_{eff})$, k_0 is the free space wavenumber, ϵ_r is the relative dielectric constant of the substrate, δ_{eff} is the effective loss tangent [5], μ_0 is the permeability of free space, $j_0(x) = \sin(x)/x$, and d_{eff} is the "effective length" of the magnetic current strip of one V/M. The concept of effective feed length and its implication are discussed in [5]. Examination of (1) and (2) indicates that the resonance occurs when $\mathrm{Re}\,(\beta_m b) \approx n\pi$, $n = 1, 2, \cdots$, or $\mathrm{Re}\,(k) \approx [(m\pi/a)^2 + (n\pi/b)^2]^{1/2}$ since $\delta_{eff} \ll 1$. We shall denote the value β_m for the particular value of n as β_{mn}, and its associated field is called the mnth mode. Clearly in the neighborhood of this resonance the field will be dominated by the term associated with β_{mn}, the value of which depends on the feed location (x', y'). Following the cavity model theory, once the field distribution is found, the Huygen source, $\mathbf{K}(x, y) = \hat{n} \times \hat{z}E(x, y)$, along the perimeter can be determined. From K, the far field can then be computed as given below:

$$E_\theta = jk_0(F_x \sin\phi + F_y \cos\phi),$$

$$E_\phi = -jk_0(F_x \cos\phi + F_y \sin\phi)\cos\theta, \quad (3)$$

where

$$F_x = \frac{d_{eff}e^{-jk_0 r}}{2\pi r} \sum_{m=0}^{\infty} A_m\{\sin(\beta_m y')e^{jk_0 b \sin\theta \sin\phi} + \sin[\beta_m(b - y')]\} \cdot \frac{jk_0 a \sin\theta\cos\phi}{(m\pi)^2 - (k_0 a \sin\theta\cos\phi)^2}, \quad (4)$$

$$F_y = \frac{bd_{eff}e^{-jk_0 r}}{2\pi r a} \sum_{m=0}^{\infty} A_m\{\sin(\beta_m b)e^{jk_0 y' \sin\theta\sin\phi} + \sin(\beta_m y')e^{jk_0 b \sin\theta\sin\phi} + \sin[\beta_m(b - y')]\} \cdot \frac{jk_0 b \sin\theta\sin\phi}{(\beta_m b)^2 - (k_0 b \sin\theta\sin\phi)^2}, \quad (5)$$

$$A_m = \frac{\cos(m\pi x'/a) j_0(m\pi d_{eff}/2a)}{\sin(\beta_m b)} [(-1)^m e^{jk_0 a \sin\theta\cos\phi} - 1]. \tag{6}$$

Also, from the field in the cavity, the ohmic and dielectric losses as well as the stored energy can be computed and finally the effective loss tangent can be determined.

III. MULTIPORT ANALYSIS

Let us consider a rectangular microstrip antenna with two ports: port 1 at (x_1, y_1) is fed with an electric current J_1, and port 2 at (x_2, y_2) is fed with a magnetic current K_2 as shown in Fig. 1. The following hybrid matrix [6] can then be used to describe the relationship between the voltage and current at these ports:

$$\begin{bmatrix} V_1 \\ I_2 \end{bmatrix} = \begin{bmatrix} h_{11} & h_{12} \\ h_{21} & h_{22} \end{bmatrix} \begin{bmatrix} I_1 \\ V_2 \end{bmatrix} \tag{7}$$

where $I_1 = d_{1eff} J_1$, d_{1eff} = effective width of source J_1, $V_2 = tK_2$ and the h parameters are given below:

$$h_{11} = -jt\omega\mu_0 \sum_{m=0}^{\infty} \cdot \frac{\cos^2(m\pi x_1/a)\cos(\beta_m y_1)\cos[\beta_m(b-y_1)]}{a\beta_m \sin(\beta_m b)} \cdot j_0^2(m\pi d_{1eff}/2a) \tag{8}$$

$$h_{12} = \frac{d_{2eff}}{a} \sum_{m=0}^{\infty} \frac{\sin[\beta_m(b-y_2)]\cos(\beta_m y_1)}{\sin(\beta_m b)} \cdot \cos(m\pi x_1/a)\cos(m\pi x_2/a) \cdot j_0(m\pi d_{1eff}/2a) j_0(m\pi d_{2eff}/2a) \tag{9}$$

$$h_{21} = -h_{12} \tag{10}$$

$$h_{22} = \frac{jd_{2eff}^2}{ta\omega\mu_0} \sum_{m=0}^{\infty} \frac{\beta_m \sin(\beta_m y_2)\sin[\beta_m(b-y_2)]}{\sin(\beta_m b)} \cdot \cos^2(m\pi x_2/a) j_0^2\left(\frac{m\pi d_{2eff}}{2a}\right). \tag{11}$$

From (8)-(11) all the z-parameters can thus be determined by the relationship between h and z parameters. Then, the input impedance at port 1, Z_{in}, can be computed:

$$Z_{in} = Z_{11} - Z_{12}^2/(Z_{22} + Z_L) \tag{12}$$

where Z_L is the load impedance across the slot terminals at (x_2, y_2). The far-field electric vector potential $\mathbf{F}$ for the two sources can be obtained by superposition as given below:

$$\mathbf{F} = \mathbf{F}_1 + P\mathbf{F}_2 \tag{13}$$

where

$$\mathbf{F}_1 = \frac{jk_0\eta t b e^{-jk_0 r}}{2\pi r} \sum_{m=0}^{\infty} \cdot \frac{\epsilon_{0m}\cos(m\pi x_1/a) j_0(m\pi d_{1eff}/2a)}{\beta_m b \sin(\beta_m b)} \cdot [(-1)^m e^{jk_0 a\sin\theta\cos\phi} - 1] \cdot \left\{ \hat{x}[\cos(\beta_m y_1) e^{jk_0 b\sin\theta\sin\phi} - \cos[\beta_m(b-y_1)]] \cdot \frac{jk_0 a\sin\theta\cos\phi}{(m\pi)^2 - (k_0 a\sin\theta\cos\phi)^2} - \hat{y}\frac{b}{a}[\beta_m b \cdot \sin(\beta_m b) e^{jk_0 y_1\sin\theta\sin\phi} + jk_0 b\sin\theta\sin\phi \cdot [\cos(\beta_m y_1) e^{jk_0 b\sin\theta\sin\phi} - \cos[\beta_m(b-y_1)]] \cdot [(\beta_m b)^2 - (k_0 b\sin\theta\sin\phi)^2]^{-1} \right\}, \tag{14}$$

$$\mathbf{F}_2 = \frac{d_{2eff} e^{-jk_0 r}}{2\pi r} \sum_{m=0}^{\infty} \frac{\cos(m\pi x_2/a) j_0(m\pi d_{2eff}/2a)}{\sin(\beta_m b)} \cdot [(-1)^m e^{jk_0 a\sin\theta\cos\phi} - 1] \cdot \left\{ \hat{x}[\sin(\beta_m y_2) e^{jk_0 b\sin\theta\sin\phi} + \sin[\beta_m(b-y_2)]] \frac{jk_0 a\sin\theta\cos\phi}{(m\pi)^2 - (k_0 a\sin\theta\cos\phi)^2} + \hat{y}\frac{b}{a}[\sin(\beta_m b) e^{jk_0 y_2\sin\theta\sin\phi} + \sin(\beta_m y_2) \cdot e^{jk_0 b\sin\theta\sin\phi} + \sin[\beta_m(b-y_2)]] \cdot \frac{jk_0 b\sin\theta\sin\phi}{(\beta_m b)^2 - (k_0 b\sin\theta\sin\phi)^2} \right\} \tag{15}$$

$$P = j\omega\mu_0 \frac{\cos(m\pi x_1/a) j_0(m\pi d_{1eff}/2a)}{\beta_m a \sin(\beta_m b)} \cdot \cos(\beta_m y_1) \cdot \cos(m\pi x_2/a)\cos[\beta_m(b-y_2)]. \tag{16}$$

From these and (3), the far field is readily computed. The analysis can be generalized for N slots in a straightforward manner.

A similar theory has been developed for a microstrip antenna with shorting pins [3]. For N pins at N ports, the impedance parameters Z_{ii} and Z_{ij} are given by

$$Z_{ii} = -jk_0 t\eta_0 \sum_{m=0}^{\infty} \frac{\epsilon_{0m}}{a}\cos^2(m\pi x_i/a) j_0^2\left(\frac{m\pi d_{ieff}}{2a}\right) \cdot \frac{\cos(\beta_m y_i)\cos[\beta_m(b-y_i)]}{\beta_m \sin(\beta_m b)} \tag{17}$$

$$Z_{ij} = -jk_0 t\eta_0 \sum_{m=0}^{\infty} \frac{\epsilon_{0m}}{a}\cos(m\pi x_i/a) \cdot \cos(m\pi x_j/a) j_0^2(m\pi d_{ieff}/2a) \cdot \frac{\cos[\beta_m(b-y_j)]\cos(\beta_m y_i)}{\beta_m \sin(\beta_m b)} \tag{18}$$

where $\eta_0 = 377\ \Omega$, $e_{0m} = 1$ for $m = 0$, and 2 otherwise, (x_i, y_i) and (x_j, y_j) are the coordinates of the source J and shorting pin, respectively. For a general case, when the N ports consist of both slots and pins as shown in Fig. 4, the currents and voltages at the N ports can also be written as follows:

$$\sum_j I_j Z_{ij} = V_i, \qquad i, j = 1, \cdots, N. \tag{19}$$

Since the solutions to E and H everywhere in the patch for any J and K have been obtained, one can therefore compute the input impedance Z_{in} at any port, using the same method as discussed above.

IV. THEORETICAL AND EXPERIMENTAL RESULTS

Our approach to the dual-frequency microstrip antenna, as stated earlier, is based on the theoretical argument that shorting pins and slots if placed at appropriate locations in the patch can raise the (0, 1) and lower the (0, 3) operating frequencies, respectively. In general, with pins and slots, the modal field is no longer pure. The existence of a substantial amount of higher order modes will modify the antenna overall resonant frequency which, as defined in [3], occurs when the reflection coefficient $|\Gamma|$ reaches a minimum.

Several antennas have been constructed and tested to determine the validity of the theory. All of them were made of double copper-clad laminate Rexolite 2200, 1/16 in thick. The relative permittivity $\epsilon_r \approx 2.62$, the loss tangent $\delta = 0.001$, and the copper cladding conductivity ≈ 270 KU. These values were used for theoretical computations.

One of the rectangular microstrip antennas, having the dimension $a = 19.4$ cm and $b = 14.6$ cm, is fed with a miniature cable at $x_1 = 9.7$ cm and $y_1 = 0$ as shown in Fig. 1. A slot of length $l = 3.0$ cm and width $w = 0.15$ cm is cut at $x_2 = 9.7$ cm and $y_2 = 7.3$ cm on the patch. The feed locations was chosen for a good match to the 50 Ω line for both F_H and F_L bands. The calculated and measured input impedance loci for both bands are shown in Figs. 2(a) and 2(b), where for comparison the corresponding loci without slot are also shown by the dashed curves. The calculated and measured radiation patterns are shown in Fig. 2(c). Similar results for slot length $l = 4.5$ cm are shown in Figs. 3(a) and 3(b). It is seen that the agreement between theoretical and measured results is excellent for both bands and that the slot has only a minor effect on the low-band impedance locus, but a significant effect on the high-band impedance locus as expected.

To further reduce the ratio of the operating frequencies of the high and low band F_H/F_L, in addition to the slots, shorting pins can be inserted along the nodal lines of the (0, 3) mode electric field as illustrated in Fig. 4. Due to limited space here, only a few typical measured impedance loci and radiation patterns for both bands are shown in Figs. 3, 5, and 6. From Figs. 3, 5, and 6, it is seen that while the "resonant" frequencies are changed for both bands with pins and slots, in general, the radiation patterns for both bands remain primarily the same. It may also be noted that the input impedance can vary widely with the feed position, and one is therefore free to choose the feed position for a desired impedance without undue concern about its effect on the pattern. The measured gains of these microstrip antennas as compared with those of a $\lambda/2$-tuned dipoles, 0.2 λ

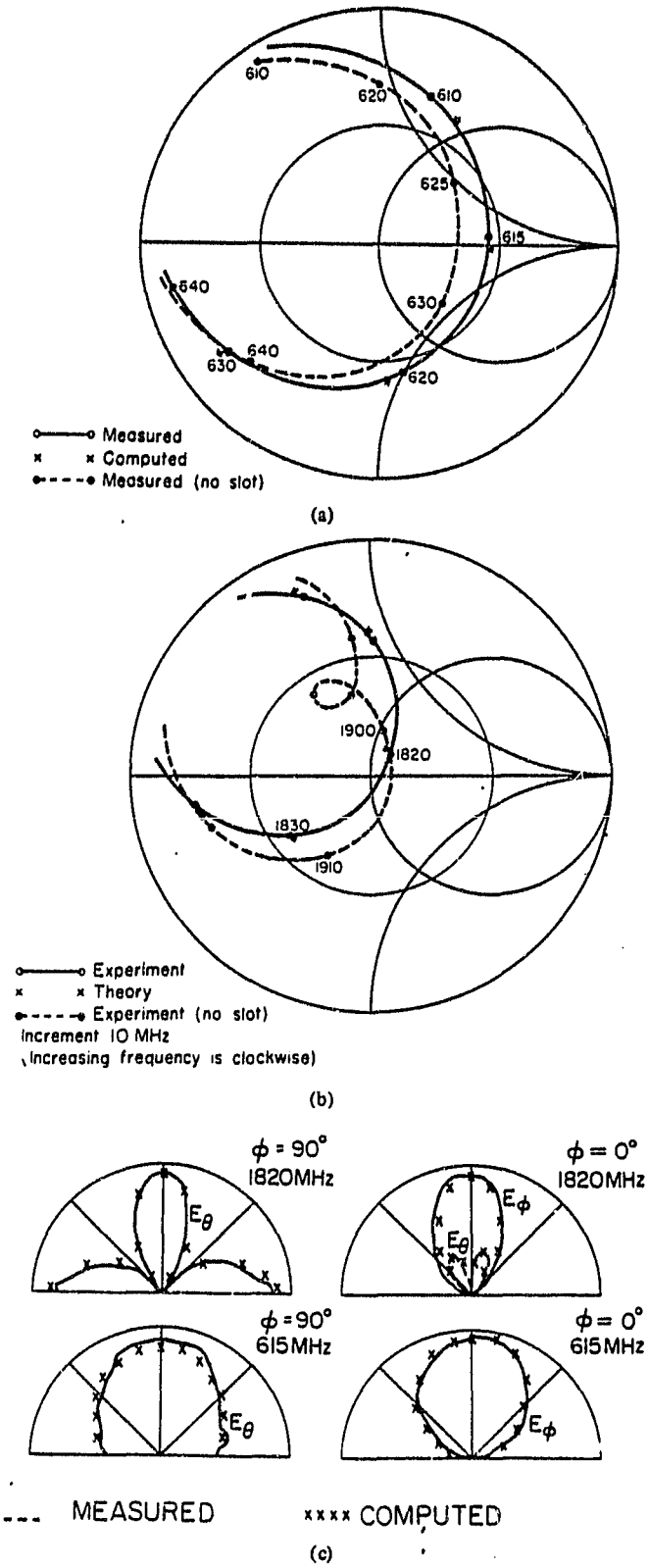

Fig. 2. (a) Measured and computed impedance loci of a rectangular microstrip antenna with one slot ($l = 3.0$ cm) for low band. $a = 19.4$ cm, $b = 14.6$ cm, and $t = 0.158$ cm. (b) Measured and computed impedance loci for high band. $a = 19.4$ cm, $b = 14.6$ cm, and $t = 0.158$ cm. (c) Measured and computed radiation patterns for both bands. $a = 19.4$ cm, $b = 14.6$ cm, and $t = 0.158$ cm.

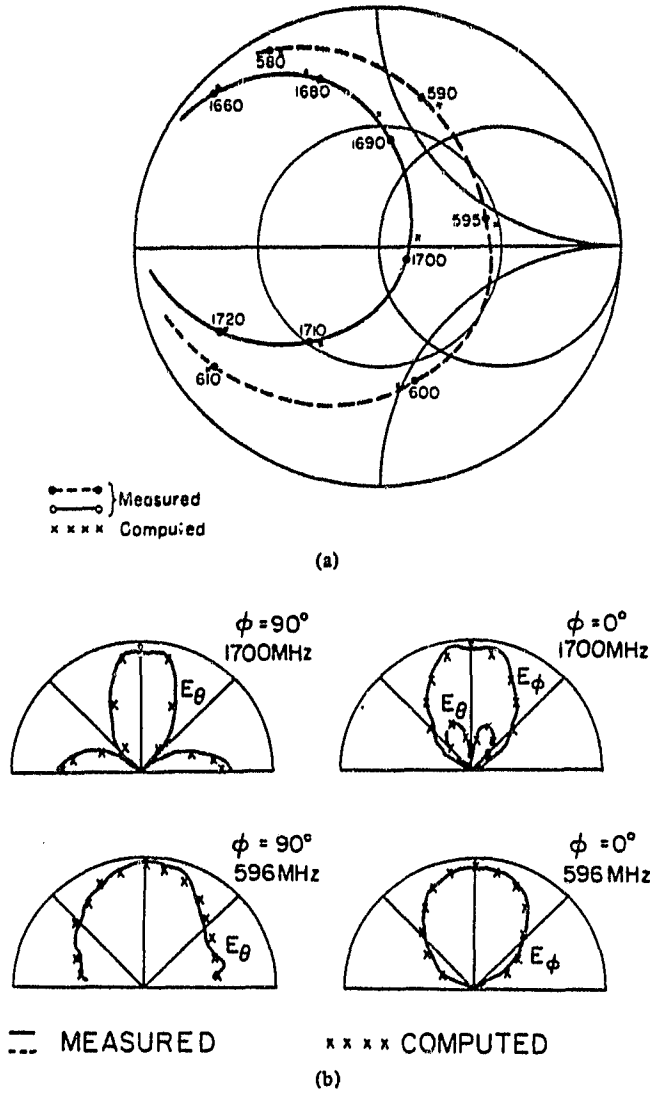

Fig. 3. (a) Measured and computed impedance loci for a rectangular microstrip antenna with one slot (l = 4.5 cm). a = 19.4 cm, b = 14.6 cm, and t = 0.158 cm. (b) Measured and computed radiation pattern for a rectangular microstrip antenna with one slot (l = 4.5 cm). a = 1.94 cm, b = 14.6 cm, and t = 0.158 cm.

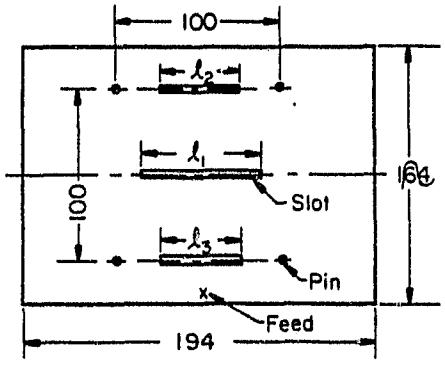

Fig. 4. The microstrip antenna with shorting pins and slots. All dimensions are in mm.

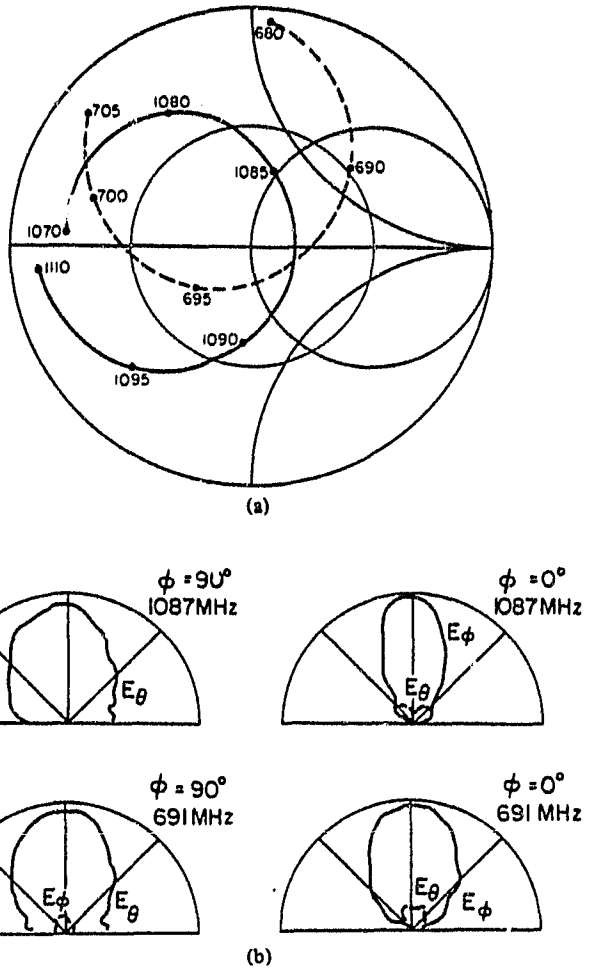

Fig. 5. (a) Measured impedance loci for a rectangular microstrip antenna with three slots and four pins. a = 19.4 cm, b = 14.6 cm, and t = 0.158 cm. (b) Measured radiation patterns for a rectangular microstrip antenna with three slots and four pins. a = 19.4 cm, b = 14.6 cm, and t = 0.158 cm.

over a ground plane are about −0.5 dB for the low band and −1.5 dB for the high band.

Table I summarizes the values of F_H/F_L for six cases. From these results, it is seen that in general the slots can lower F_H and shorting pins raise F_L, resulting in a variation of F_H/F_L from 3.02 to 1.31. In fact, this ratio can be reduced even further by adding more pins and slots. However the effectiveness of adding more pins and shots will eventually diminish. Instead, we find that the ratio F_H/F_L can be reduced to about 1.07 by using a C-shaped slot (or a wrapped around microstrip line). This will be reported elsewhere.

V. CONCLUSION

This investigation shows that a single rectangular microstrip antenna element can be designed to perform for dual-frequency bands corresponding approximately to the (0, 1) and (0, 3) modes. The frequencies of both bands can be tuned over a wide range, with their ratio from 3 to less than 1.3, by adding shorting pins and slots in the patch. A method for analyzing these antennas has been developed and treats the antenna as a multiport cavity. The validity of this theory is verified by comparing the computed impedance loci and radiation patterns with the measured for a few simple cases.

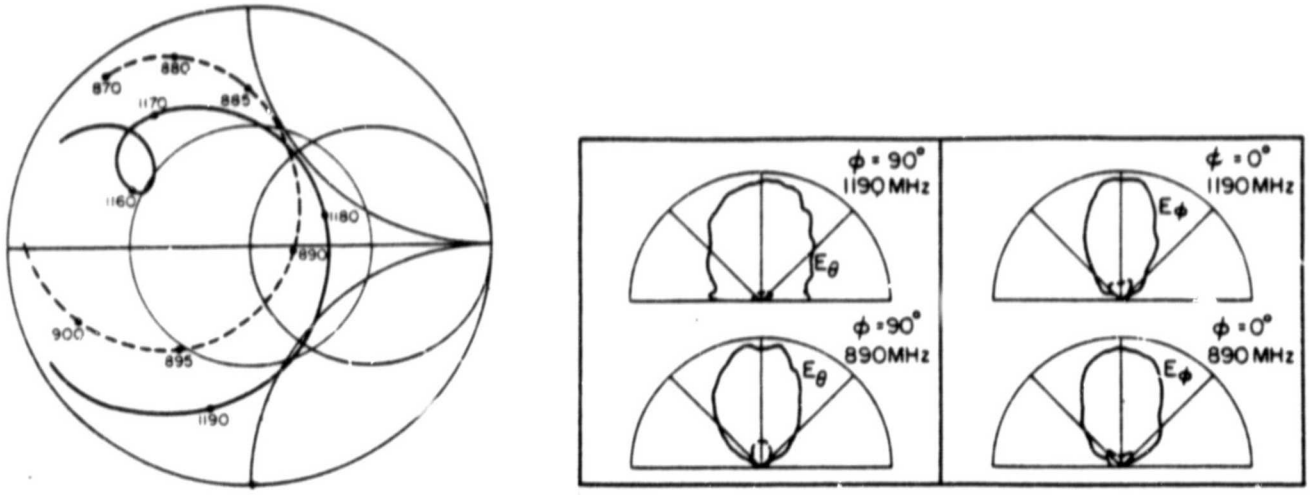

Fig. 6. (a) Measured impedance loci for a rectangular microstrip antenna with three slots and ten pins. a = 19.4 cm, b = 14.6 cm, and t = 0.158 cm. (b) Measured radiation pattern for a rectangular microstrip antenna with three slots and ten pins. a = 19.4 cm, b = 14.6 cm, and t = 0.158 cm.

TABLE I
OPERATING FREQUENCIES FOR BOTH F_L AND F_H

CASE	F_L(MHz)	F_H(MHz)	F_H/F_L
A. One slot ℓ_1 = 1.0 cm at (9.7,7.3)	628	1900	3.02
B. One slot ℓ_1 = 3.0 cm at (9.7,7.3)	596	1700	2.85
C. Three slots ℓ_1 = 7.0 cm ℓ_2 = ℓ_3 = 3.0 cm at (9.7,2.4), (9.7,7.3) and (9.7,12.2)	555	1420	2.55
D. Three slots ℓ_1 = ℓ_2 = ℓ_3 = 7.0 cm at the same location as in case C.	553	1310	2.36
E. Same as case D but with four pins as shown in Figure 2.	698	1087	1.56
F. Same as case E with six additional pins at (3.7,2.4), (9.7,2.4), (15.7,2.4), (3.7,12.2), (9.7,12.2) and (15.7,12.2)	890	1181	1.31

As a design guide, in general, the effect of slot on the high-band frequency is stronger if it is placed where the high-order modal magnetic field is stronger, and the effect of short pin on the low-band frequency is stronger if it is placed where the low-order modal electric field is stronger.

REFERENCES

[1] G. G. Sanford, and R. E. Munson, "Conformal VHF antenna for the Apollo-Soyuz test project," in *IEEE Antennas Propagat. Int. Symp. Digest*, Oct. 1976.

[2] A. G. Derneryd, "Microstrip disc antenna covers multiple frequencies," *Microwave J.*, pp. 77-99, May 1978.

[3] Y. T. Lo, C. E. Skupien, and S. S. Zhong, "A study of microstrip antennas for multiple band operation," Rep. RADC-TR-82-236, Sept. 1982. (Also Y. T. Lo, C. E. Skupien, S. S. Zhong, and W. F. Richards, "Dual-frequency microstrip antennas," in *1983 Nat. Radio Sci. Meeting Digest*, URSI, Houston, TX, p. 98, and D. H. Schaubert, F. G. Garrar, A. Sindoris, and S. T. Hayes, "Microstrip antennas with frequency agility and polarization diversity," *IEEE Trans. Antennas Propagat.*, vol. 29, pp. 118-123, Jan. 1981 for using shorting post for tuning.)

[4] W. F. Richards, Y. T. Lo, and D. D. Harrison, "An improved theory for microstrip antennas and applications," Rep. RADC-TR-79-111, May 1979, and *IEEE Trans. Antennas Propagat.*, vol. AP-29, no. 1, Jan. 1981.

[5] Y. T. Lo, W. F. Richards, P. C. Simons, J. E. Brewer and C. P. Yuan, "Study of microstrip antenna elements, arrays, feeds, losses and applications," Rep. RADC-TR-81-98.

[6] C. A. Desorer and E. S. Kuh, *Basic Circuit Theory*. New York: McGraw-Hill, 1969.

Bao F. Wang was born in Tienjing, China, on July 15, 1938. He received the B.S. degree in electrical engineering from Beijing Aeronautics and Astronautics Institute, Beijing, China, in 1961.

From 1961 to 1969 he was on the faculty of the Department of Radio Engineering, Beijing Aeronautics and Astronautics Institute. From 1969 until 1982 he worked in the Microwave Technique Laboratory of the same institute and developed various airborne remote control and remote sensing antennas, circularly polarized horn antennas, slot antennas, helical antennas, and microstrip antennas. Since January 1983 he has been a visiting scholar at the Electromagnetics Laboratory, University of Illinois at Urbana-Champaign, under Professor Y. T. Lo working on the dual-frequency microstrip antennas and the coupling problems between multiple ports in a microstrip antenna.

Yuen T. Lo (S'49-A'53-M'58-SM'66-F'69), for a photograph and biography please see page 46 of the January 1981 issue of this TRANSACTIONS.

CIRCULARLY POLARIZED MICROSTRIP ANTENNAS

Y. T. Lo
B. Engst

Electromagnetics Laboratory
University of Illinois
Urbana, IL

R. Q. H. Lee

Lewis Research Center
NASA
Cleveland, OH

I. Introduction

It is well known that a simple microstrip antenna can be made to radiate EM waves of any polarization, in particular, the circular polarization (CP) without any phasing network and power divider [1 - 5]. A simple but surprisingly accurate theory for this family of antennas has been developed and reported in the 1979 Antenna Applications Symposium. However, the CP bandwidth, (CPBW) namely the bandwidth in which the axial ratio (AR) is less than a certain specified value, say 3 dB, is very small. For example, for a nearly square patch made of 1/16" thick Rexolite 2200 and designed to operate at 800 MHz, the CP bandwidth is only about 0.3%. Most of those experimental designs were made for a feed placed along the diagonal of the patch. But the theory shows that there are practically infinitely many possible designs with different feed locations [3 - 5]. The purposes of this paper are: first to clear up the speculation that other designs might give a wider bandwidth, and second to show an effective method for broadening the bandwidth.

II. Theory

First we briefly review the theory for CP microstrip antennas [3]. For concreteness, let us consider a rectangular patch with effective dimensions $a \times b$, relative substrate dielectric constant ε_r, and effective loss tangent δ_{eff} which can be either computed or simply measured from the Q-factor of the antenna. In general, an infinite number of modes will be excited. However, as the excitation frequency ω is near the resonant frequency of one of the modes, say the mnth mode:

$$\omega \approx \omega_{mn} = \left\{ \frac{1}{\mu_o \varepsilon_o \varepsilon_r} \left[\left(\frac{m\pi}{a} \right)^2 + \left(\frac{n\pi}{b} \right)^2 \right] \right\}^{1/2} = \frac{1}{\sqrt{\mu_o \varepsilon_o \varepsilon_r}} k_{mn} \qquad (1)$$

the mnth modal field will overwhelmingly dominate over all others, particularly for thin microstrip antennas. The radiated field is then found to be inversely proportional to $(k - k_{mn})$ where $k = \omega\sqrt{\mu_o\varepsilon_o\varepsilon_r(1 - j\delta_{eff})} \approx k_o\sqrt{\varepsilon_r}(1 - j\delta_{eff}/2) \approx k_o\sqrt{\varepsilon_r}(1 - j/2Q) \approx k' + jk''$. Now let us consider a nearly square patch, namely $0 < a - b \approx c \ll a$ and b; then for the two dominant modes,

$$k_{01} \approx \pi/b \approx k_{10} \approx \pi/a \quad . \tag{2}$$

If the excitation frequency is such that

$$k_{10} < k' < k_{01} \quad , \tag{3}$$

then the fields associated with both of these modes will be strongly excited. Let the normal of the patch be the z-axis, the patch side having dimension a be along the x-axis and b along the y-axis. The radiated field along the z-axis will have two orthogonal components whose ratio is approximately given by

$$\frac{E_y}{E_x} \approx A\,\frac{k - k_{10}}{k - k_{01}} \tag{4}$$

where

$$A \approx \frac{\cos(\pi y'/b)}{\cos(\pi x'/a)} \tag{5}$$

$$(x',y') \approx \text{coordinates of the feed location} \quad . \tag{6}$$

If a, b, x', and y' are such that

$$E_y/E_x \approx \pm j \quad , \tag{7}$$

then LH and RH CP will be obtained, respectively. To see how the design parameters a, b, x', and y' are related, it is not only the simplest but also the most illuminating method by examining (4) and (7) in the k-plane as shows in Figure 1.

For LHCP the phasor $(k - k_{10})$ must lead $(k - k_{01})$ by $\pi/2$ and the ratio of their lengths must be equal to $1/A$. For given a and b, the solution for k' is given by the intersection of the circle whose diameter is $(k_{01} - k_{10})$ and center at $(0,(k_{01} + k_{10})/2)$ and the line $k''/k' = -1/2Q$. Clearly these are three possibilities: (1) no solution if $(k_{01} - k_{10}) < 2k'' = k'/Q = k_{10}/Q$; (2) one solution if $(k_{01} - k_{10}) = 2k'' = k_{10}/Q$; and (3) two solutions if $(k_{01} - k_{10}) > 2k'' = k_{10}/Q$.

Let us consider the last case first. Using the similarity of triangles one readily obtains the following:

$$\frac{p}{|k - k_{10}|} = \frac{|k''|}{|k - k_{01}|} \quad \Rightarrow \quad p = |k''|/A \tag{8}$$

$$\frac{q}{|k - k_{01}|} = \frac{|k''|}{|k - k_{10}|} \quad \Rightarrow \quad q = |k''|A \tag{9}$$

where p and q are $(k' - k_{10})$ and $(k_{01} - k')$, respectively, as indicated in Figure 2, and

$$A = |k - k_{01}|/|k - k_{10}| \tag{10}$$

as from (4) and (7). One of the two possible solutions for k' is

$$k' = k_{10} + p = k_{10} + \frac{k'}{2QA} \quad \Rightarrow \quad \boxed{k' = k_{10}/\left(1 - \frac{1}{2QA}\right)} \; . \tag{11}$$

Furthermore,

$$k_{01} - k_{10} = p + q = |k''|\left(A + \frac{1}{A}\right) = \frac{k'}{2Q}\left(A + \frac{1}{A}\right) . \tag{12}$$

From (11) and (12), one obtains an equation for A:

$$\boxed{A^2 - \frac{2Qc}{b} A + \left(1 + \frac{c}{b}\right) = 0} \tag{13}$$

Thus there are, in general, two possible solutions for A which will be denoted by A_1 and A_2. From (13)

$$A_1 A_2 = 1 + \frac{c}{b} \approx 1 \quad . \tag{14}$$

Thus, when $c \ll b$ if A_1 is a solution, so is $1/A_1$. The latter when substituted into (11) gives the corresponding second solution of k':

$$k' = k_{10} \Big/ \left(1 - \frac{A}{2Q}\right) . \tag{15}$$

Equations (13) and (11) are the two basic design formulas. For example, for a given material and given dimensions a and b, Q can be either computed or measured [3]. Then (13) is solved for the two solutions of A, each of which determines the feed locus and its corresponding frequency from (11). Since for $c \ll b$, $A_1 A_2 \approx 1$, the two loci for the two frequencies are approximately symmetrical with respect to the line $x = y$.

For RHCP, the lower sign of (7) should be used. Then by defining

$$A = - \frac{\cos(\pi y'/b)}{\cos(\pi x'/a)} \tag{16}$$

all the above derivations and, therefore, all the above results remain unchanged. In other words the feed loci for RHCP are simply the reflections of those for LHCP with respect to the line $x = a/2$, or $y = b/2$. These will be demonstrated later in some examples.

For the special case $A_1 = A_2 = 1$, i.e., the feed is along the diagonal line $y'/x' = b/a$, (13) reduces to

$$\frac{a}{b} = \frac{2Q + 1}{2Q - 1} \approx 1 + \frac{1}{Q} + \frac{1}{2Q^2} \quad . \tag{17}$$

and the circle in Figure 1 becomes tangent to the line $k''/k' = -1/2Q$.

IV. Numerical and Experimental Results

Several experimental patch antennas were designed and tested. All of them were made of Rexolite 2200 with $\epsilon_r = 2.62$ and dielectric loss tangent 0.001. One of them has the following physical dimensions:

$$a = 16.1 \text{ cm}, \quad b = 15.9 \text{ cm}, \quad t = 0.32 \text{ cm} \quad .$$

Past results show that the effective values of a and b are about 1.5t larger than the actual physical dimensions. The Q of this patch is found to be about 100. Using (13) the four feed loci, two at f_1 and f_2 for LHCP and two others also at f_1 and f_2 for RHCP were computed and plotted in Figure 2. The patterns measured with a rotating dipole for feed points 1 and 2 at 597 MHz and 590.4 MHz, respectively, are shown in Figures 3(a) and 3(b). These patterns are about the same as those reported earlier for the patches designed for A = 1. For the feed at point 2, the AR vs. f is listed in Table 1. The CP bandwidth is about 0.5%. An attempt to broaden the bandwidth by feeding the patch at a compromise point between points 1 and 2 was found ineffective and sometimes resulting in worse AR. The input impedance characteristic for feed at 1 and 2 are shown in Figures 4(a) and 4(b).

V. Broadbanding of CP Microstrip Antennas

Assuming that the dimensions of a CP patch antenna have been determined by using the design formula given above, one can then compute the CP bandwidth by using (4) as the frequency, or k', departs from the designed value until the AR becomes 3 dB. Using this method we have previously shown that the CP bandwidth is approximately (35/Q) percent for Rexolite 2200 [3]. Thus to broaden the

bandwidth, Q must be lowered. This can only be achieved effectively by using thick substrate [6]. Unfortunately, so far there is no theory available for thick CP microstrip antennas, nor a precise knowledge about the upper limit of the substrate thickness beyond which the cavity-model theory breaks down. Under this circumstance we simply used the latter theory to design several patch antennas with thickness as much as 0.053 λ_o, (λ_o = free space wavelength) or 0.084 λ, (λ = substrate dielectric wavelength). To our surprise excellent results could still be obtained. This is discussed below with several examples.

(a) The first patch, designed to operate in the 10 GHz range, has the following physical dimensions:

$a = 0.946$ cm, $b = 0.911$ cm, $t = 0.08$ cm

and its Q-factor is found to be about 20. Using (13) one finds that the proper feed location is along the diagonal of the patch. For a good match to the 50 Ω line, the feed coordinates are chosen to be

$x' = 0.21$ cm, $y' = 0.2$ cm

The measured patterns at 10.22 GHz in the two planes $\phi = 0°$ and 90° are shown in Figures 5a. Excellent AR is observed over a wide angular region. Figures 5b - 5c show the patterns in the $\phi = 0°$ plane at the two edge frequencies, 10.306 and 10.16 GHz, of the CP bandwidth, which is about 1.44%, substantially larger than that obtained earlier for the thin substrate. But in this case $t \approx 0.044\ \lambda$.

(b) The second patch has the following physical dimensions:

$a = 0.964$ cm, $b = 0.859$ cm, $t = 0.16$ cm

Its Q is found to be 8 and $(x',y') = (0.3, 0.28)$ cm. The patterns for 9.74 GHz in the two principal planes and for the two edge frequencies, 9.9 and 9.577 GHz,

of the CP band in the $\phi = 0°$ plane are shown in Figures 6a - 6c. For this thick substrate, the CPBW is about 3.3%.

All of these results as well as a few others are summarized in Table 2. The CP bandwidth vs. t in λ or λ_o is plotted in Figure 7. It is interesting to note that their relationship is nearly linear and can be given approximately by

$$\text{CPBW}(\%) \approx 36.7t(\lambda) + 0.16 \quad \text{for } t > 0.005\ \lambda \quad .$$

Earlier we showed that the CPBW (in %) is approximately equal to 35/Q. This is plotted in Figure 8 where the experiment results are also marked. The agreement is surprisingly good.

(c) The last example has the physical dimensions

$$a = 1.088 \text{ cm}, \quad b = 0.90 \text{ cm}, \quad t = 0.08 \text{ cm} \quad .$$

These dimensions result a feed point at $x' = 0.2$ cm, $y' = 0.39$ cm which is not on the diagonal line. The patterns are shown in Figures 9a - 9c for $f = 10.27$, 10.18, and 10.36 GHz, the latter two being the edge frequencies of the CPBW of about 1.75%. The small improvement of this BW over that of the design (a) with the feed along the diagonal line is probably within our experimental error and should not be taken seriously.

VI. Conclusions

(1) Despite the fact that our CP microstrip antenna theory is based on the cavity model, valid only for thin substrate, this investigation shows that it is still applicable for substrate as thick as 0.084 of a dielectric wavelength.

(2) The CP bandwidth of a microstrip antenna depends mainly on its Q-factor, thus its thickness. A CPBW of 3% can be obtained if the substrate is about 8% of a dielectric wavelength thick. For this case $Q \approx 8$, indicating a very good radiation efficiency.

(3) For a fixed thickness, the CPBW cannot be broadened significantly by using other designs. However, other designs do provide a means for moving the feed from one point to some other point which may be necessary, due to some packaging problem.

VII. References

[1] H. D. Weinschel, "A cylindrical array of circularly polarized microstrip antennas," IEEE AP-S International Symposium Digest, pp. 175-180, June 1975, Urbana, IL.

[2] J. L. Kerr, "Microstrip polarization techniques" Proc. of the 1978 Antenna Applications Symposium at Allerton Park, University of Illinois, Urbana, IL.

[3] Y. T. Lo, W. F. Richards, and D. D. Harrison, "An improved theory for microstrip antennas and applications - Part I," Interim Report, RADC-TR-79-111, May 1979; also W. F. Richards, Y. T. Lo and D. D. Harrison, "An improved theory for microstrip antennas and applications," IEEE Trans., AP-29, pp. 38-46, Jan. 1981.

[4] W. F. Richards, Y. T. Lo, and P. Simon, "Design and theory of circularly polarized microstrip antennas," IEEE AP-S International Symposium Digest, pp. 117-120, June 1979.

[5] Y. T. Lo and W. F. Richards, "A perturbation approach to the design of circularly polarized microstrip antennas," IEEE AP-S Inernational Symposium, pp. 339-342, June 1981.

[6] Y. T. Lo, et al., "Study of microstrip antenna elements, arrays, feeds, losses, and applications," Final Technical Report, RADC-TR-81-98, June 1981.

Acknowledgement

This work is supported by Lewis Research Center, NASA, Cleveland, OH and RADC Hanscom AFB, MA.

TABLE 1.

AR vs. frequency of the microstrip antenna shown in Figure 2 and fed at point 2: $x' = 6.75$ cm, $y' = 5.1$ cm

f (MHz)	AR (dB)
588.96	3
589.3	2.5
589.8	1.5
590.4	1
591.2	1.4
591.8	2.7
592	3

TABLE 2.

Measured CP bandwidths for various substrate thicknesses t

f (GHz)	λ_o (cm)	t(cm)	$t(\lambda_o)$	$t(\lambda)$	CPBW(%)	Q
0.59	50.85	0.16	0.0032	0.0051	0.35	130
0.59	50.85	0.32	0.0063	0.01	0.5	100
1.200	25	0.32	0.0128	0.021	0.84	58
10.22	2.935	0.08	0.0273	0.044	1.44	20
9.74	3.093	0.16	0.053	0.084	3.3	8

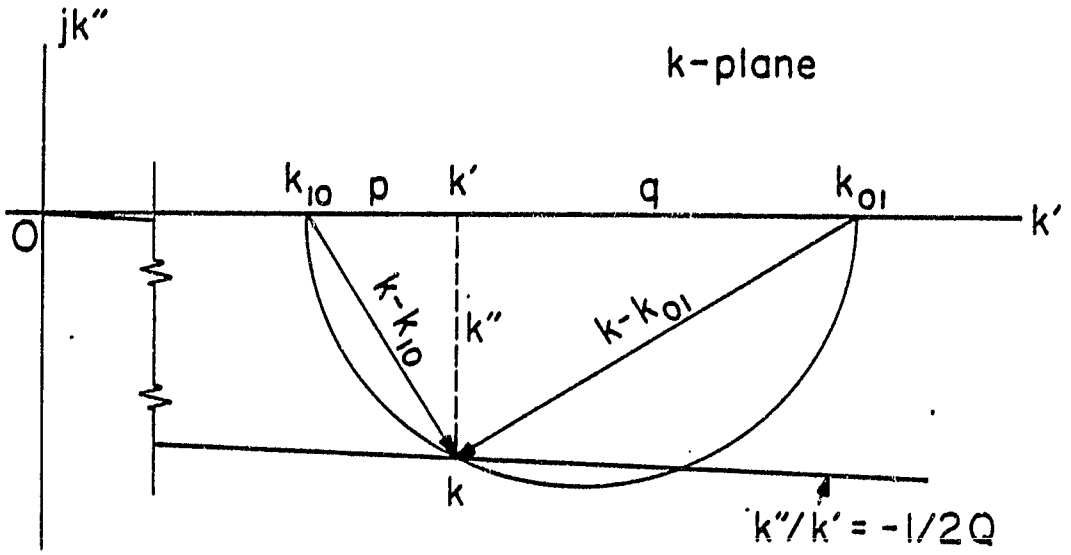

$$k = k' + jk''$$

Figure 1. Geometric relations of phasors k_{10}, k_{01} and k in k-plane for CP operation.

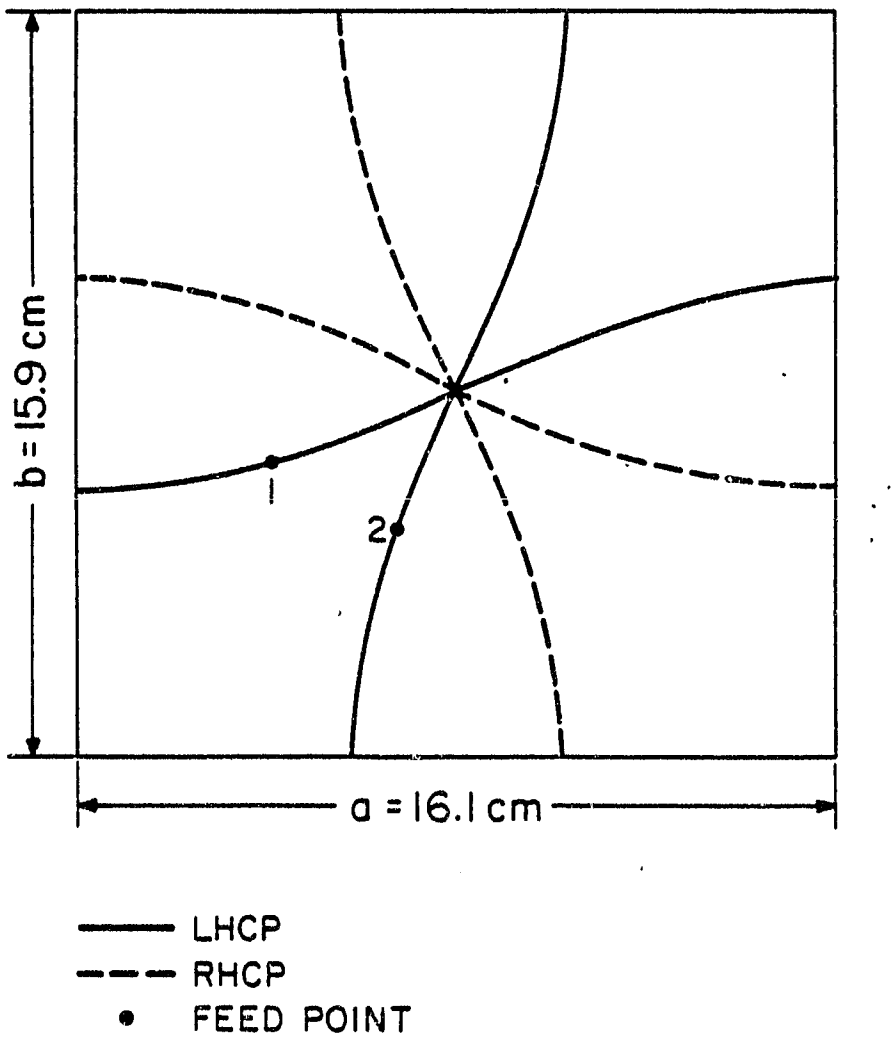

Figure 2. Feed loci for a rectangular CP microstrip antenna with substrate thickness 0.32 cm and relative dielectric constant 2.62.

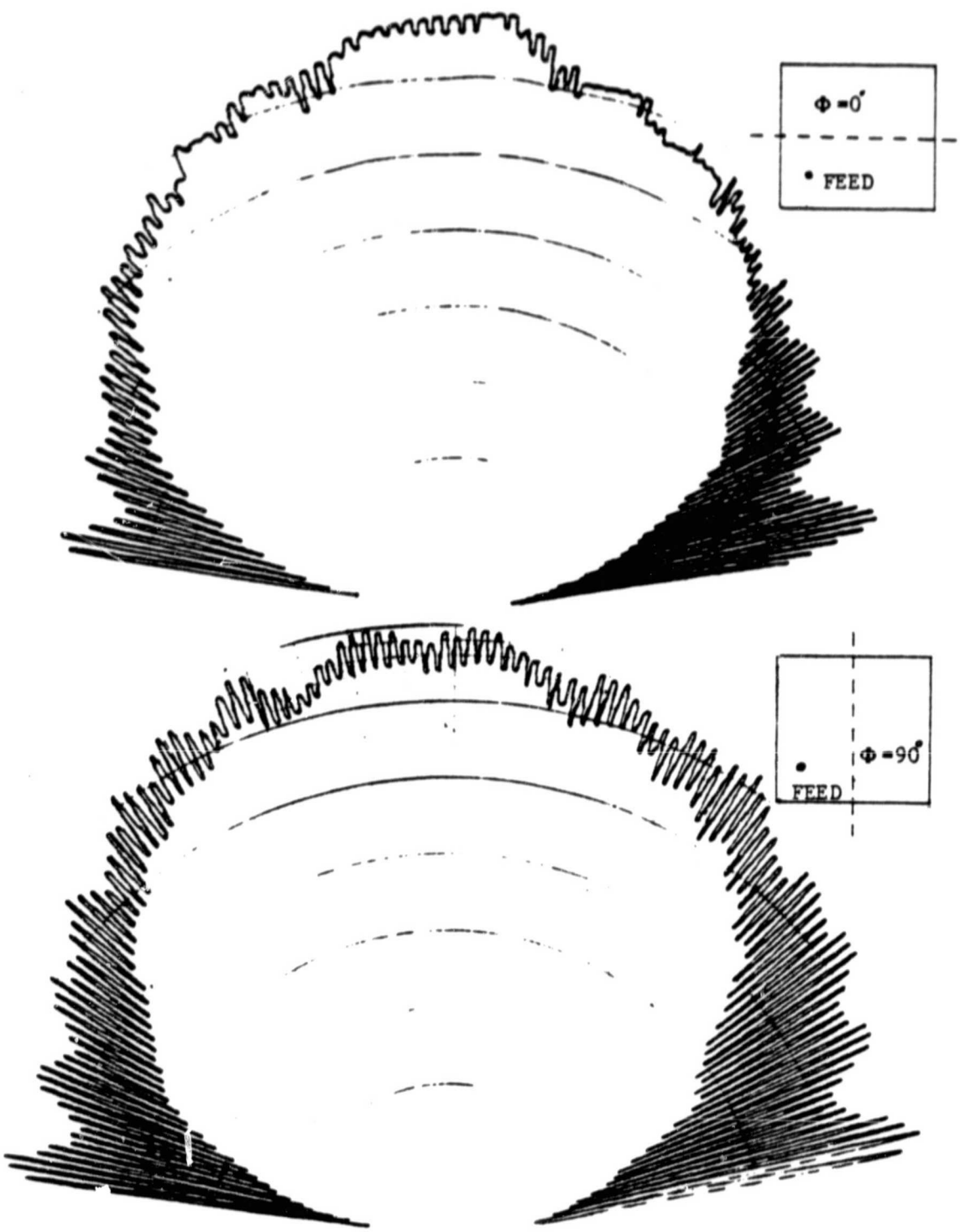

Figure 3(a). Field patterns in principal planes of the microstrip antenna shown in Figure 2, at point 1: x' = 4.55 cm, y' = 6.37 cm, and f = 597 MHz.

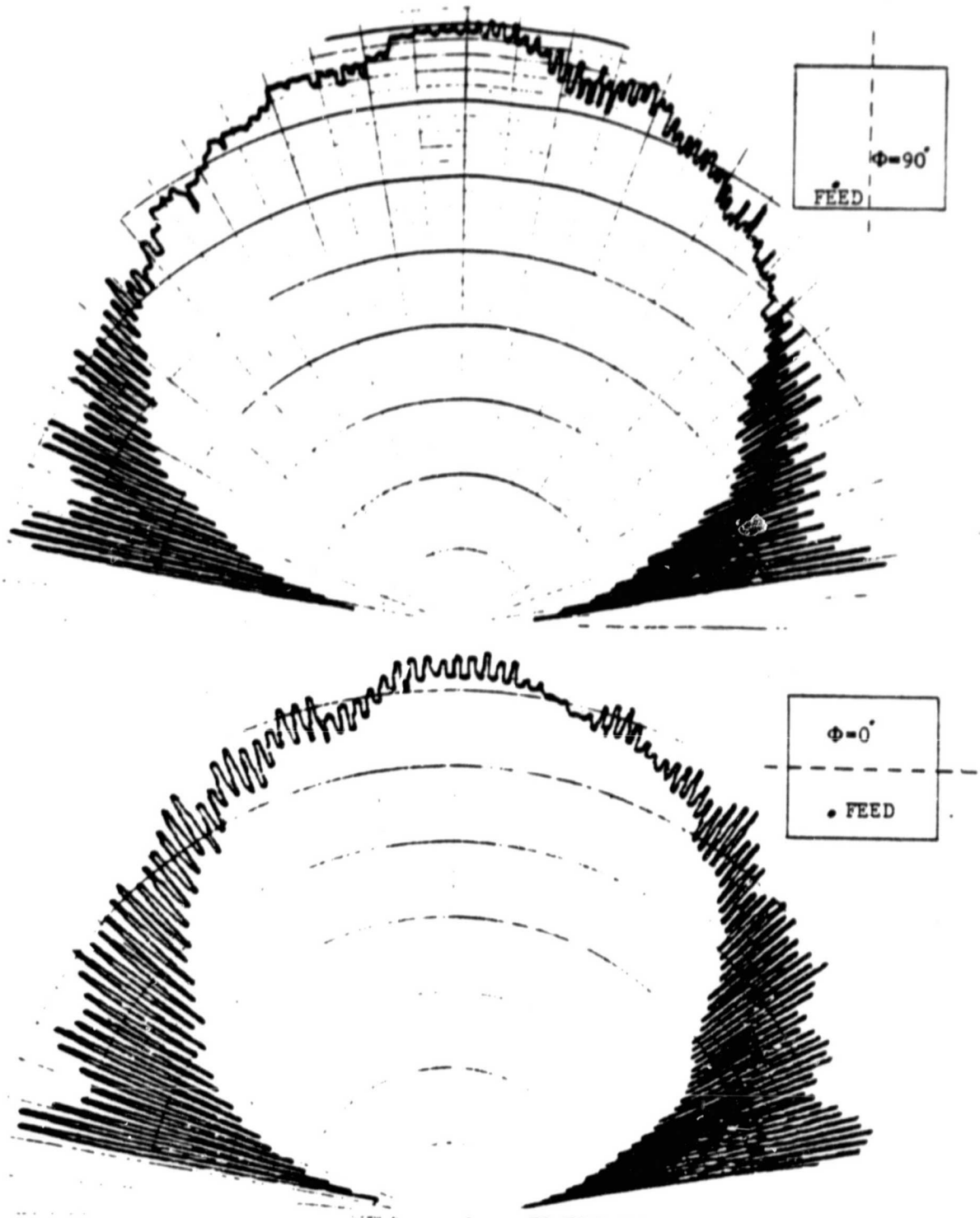

Figure 3(b). Field patterns in principal planes of the microstrip antenna shown in Figure 2, at point 2: x' = 6.75 cm, y' = 5.1 cm, and f = 590.4 MHz.

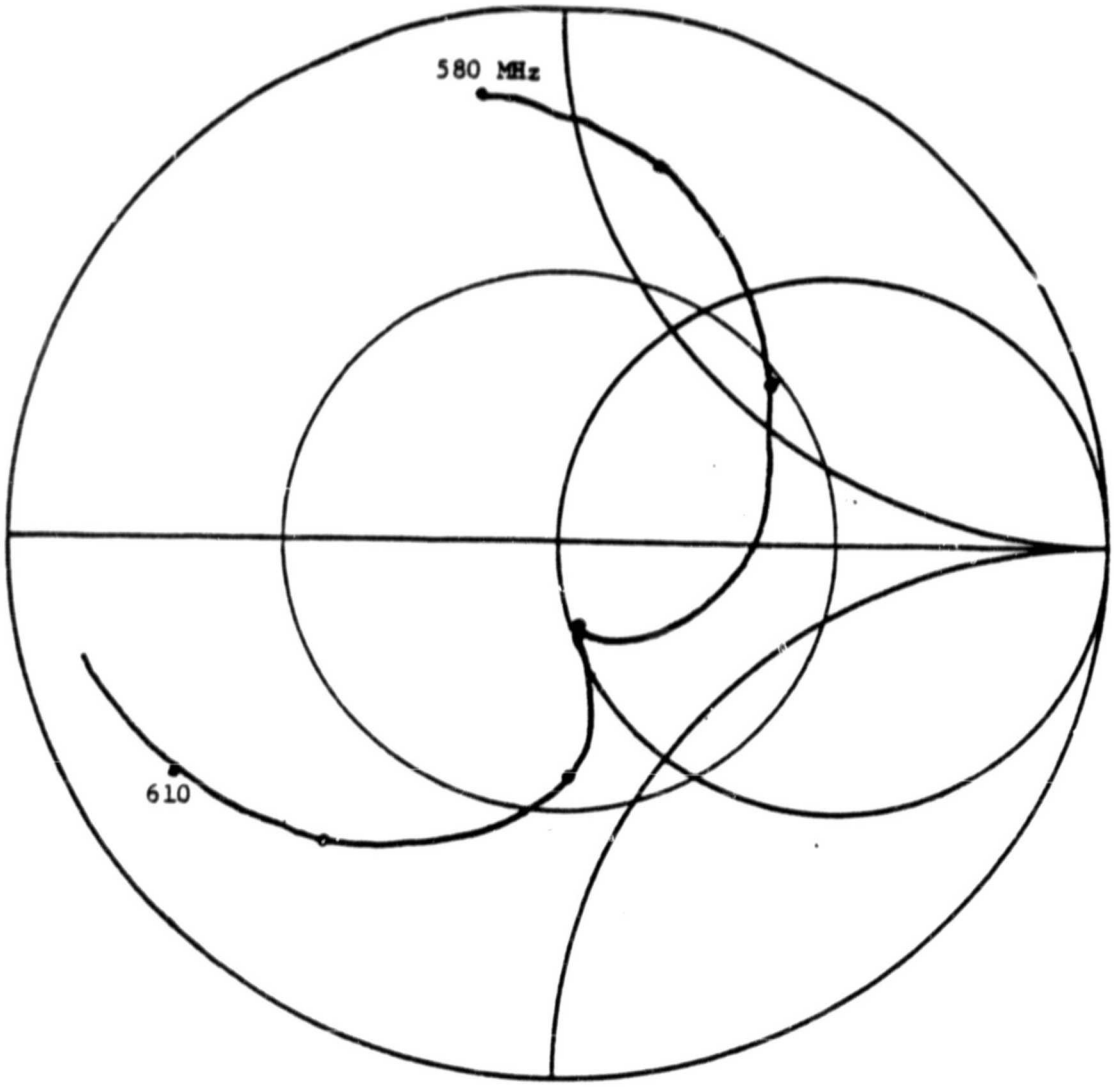

a) Impedance locus, frequency increment = 5 MHz.

Figure 4. Input impedance of the antenna shown in Figure 2 and fed at point (a) 1 and (b) 2.

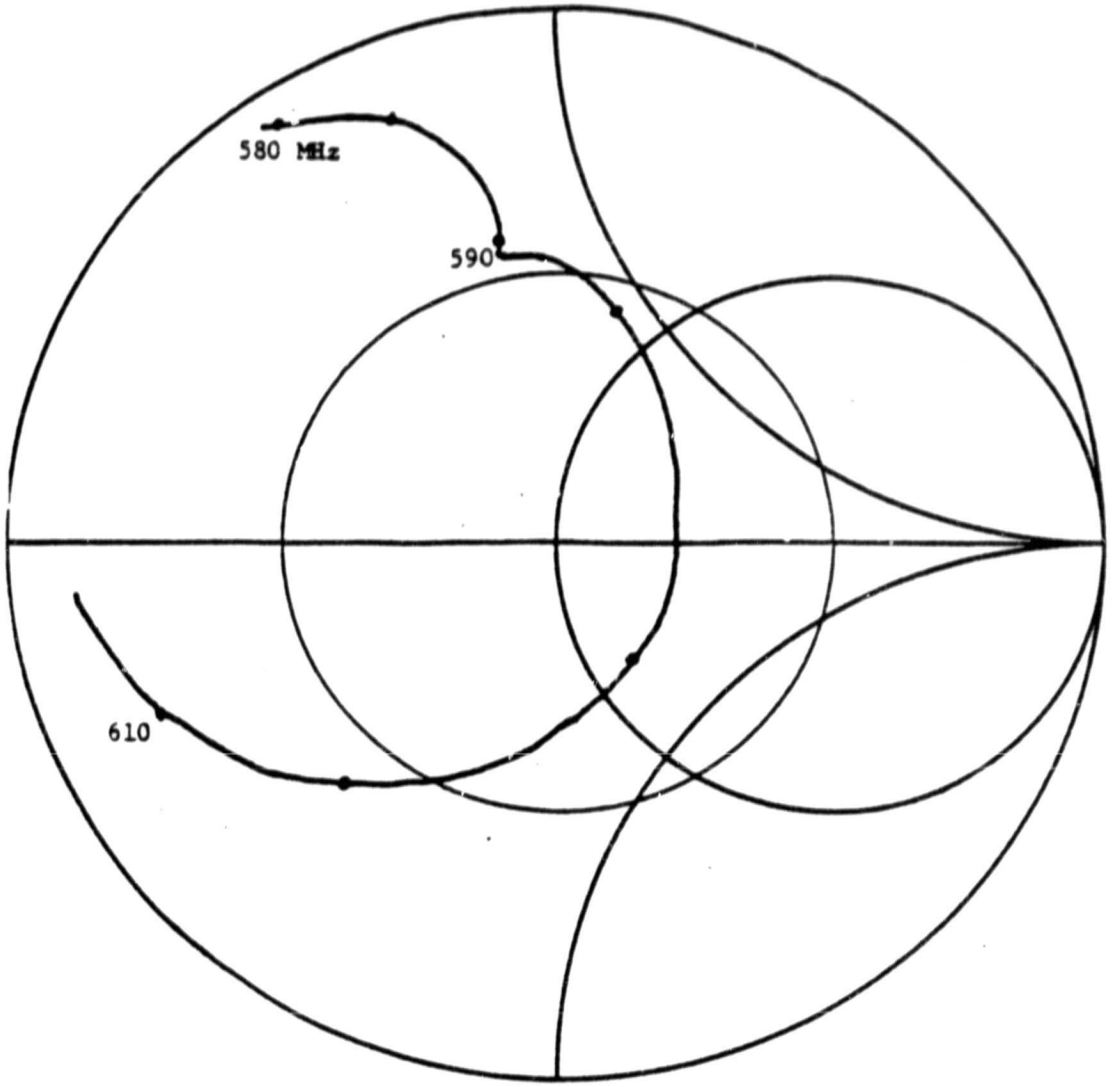

b) Impedance locus, frequency increment = 5 MHz.

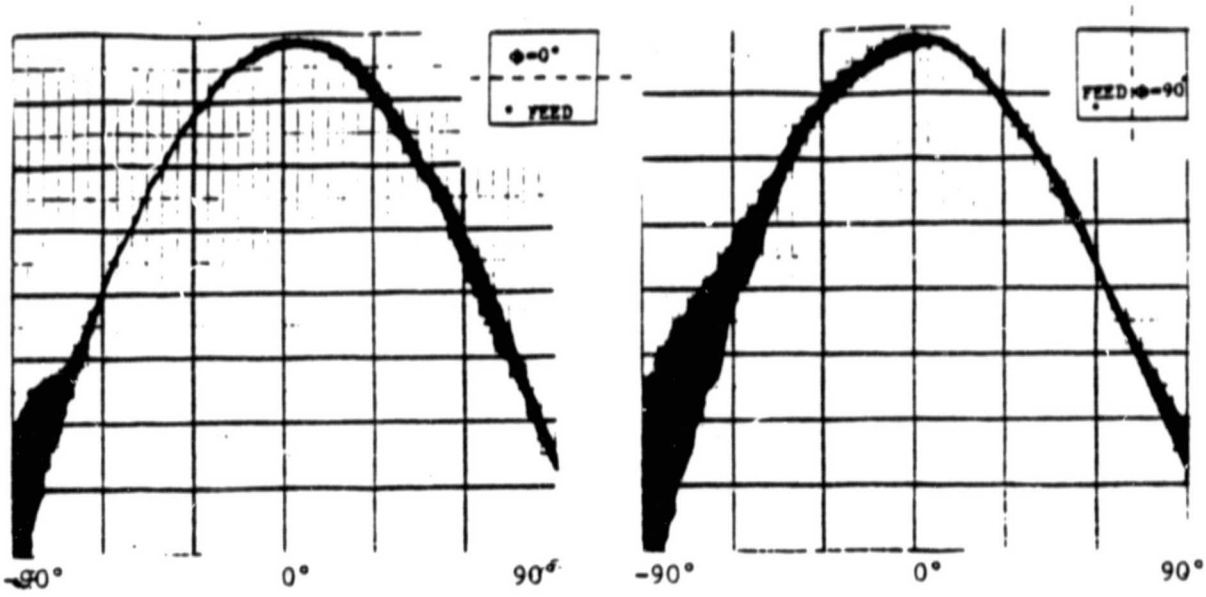

a) f=10.22 GHz

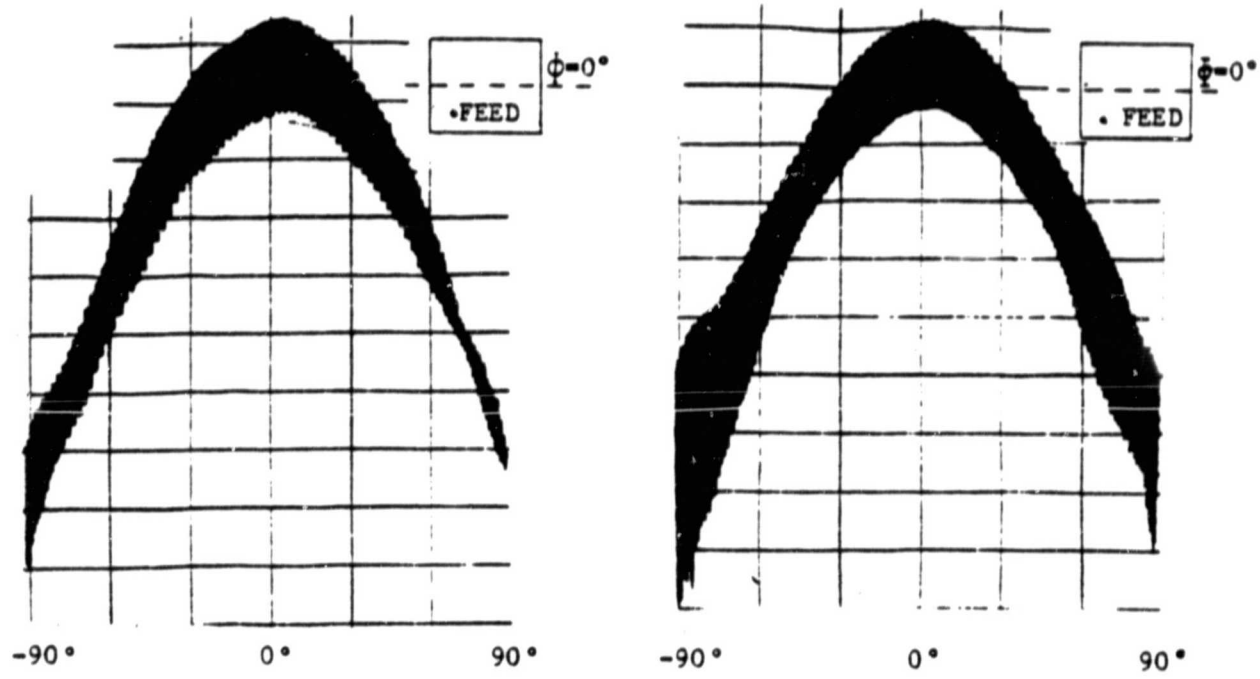

b) f=10.306GHz

c) f=10.16GHz

Figure 5. Field patterns in principal planes shown of the micrstrop antenna with dimension a = 0.946 cm, b = 0.911 cm, t = 0.08 cm, and feed point at x' = 0.21 cm, y' = 0.2 cm.

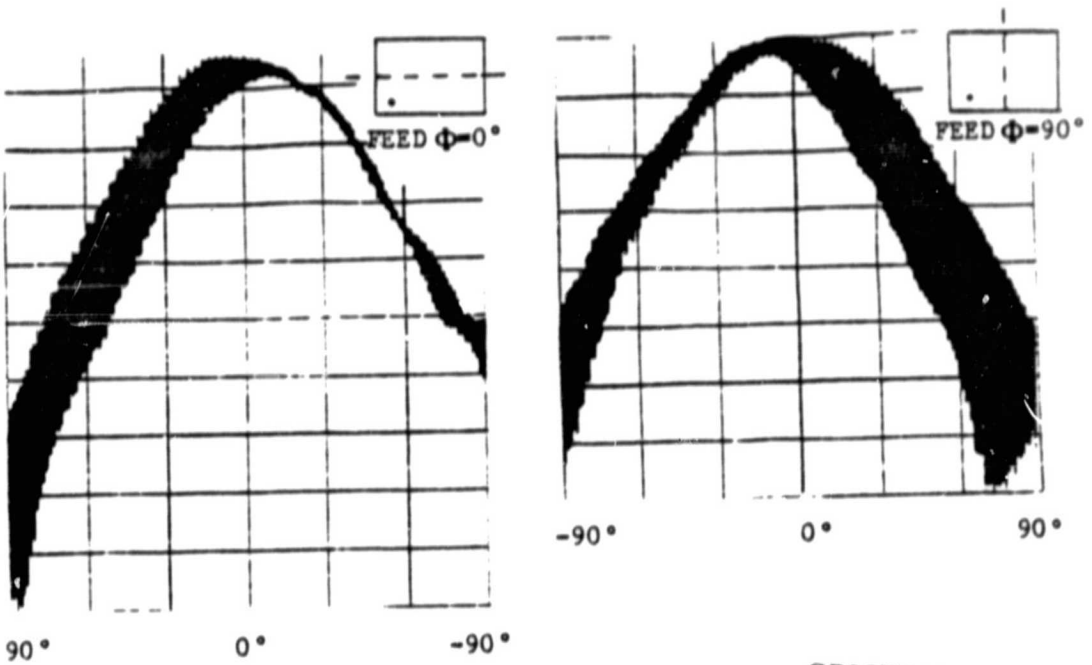

a) f=9.74GHz

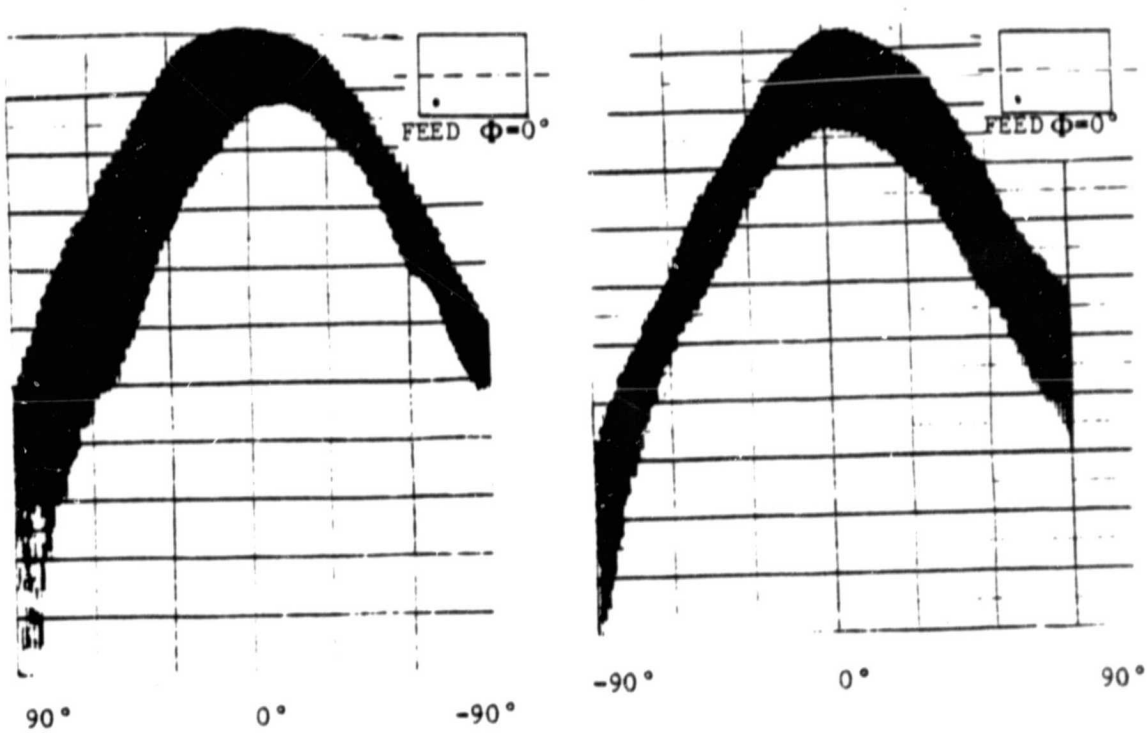

b) f=9.9GHz

c) f=9.577GHz

Figure 6. Field patterns in principal planes shown of the microstrip antenna with dimension a = o.964 cm, b = 0.859 cm, t = 0.16 cm, and feed point x' = 0.3 cm, y' = 0.28 cm.

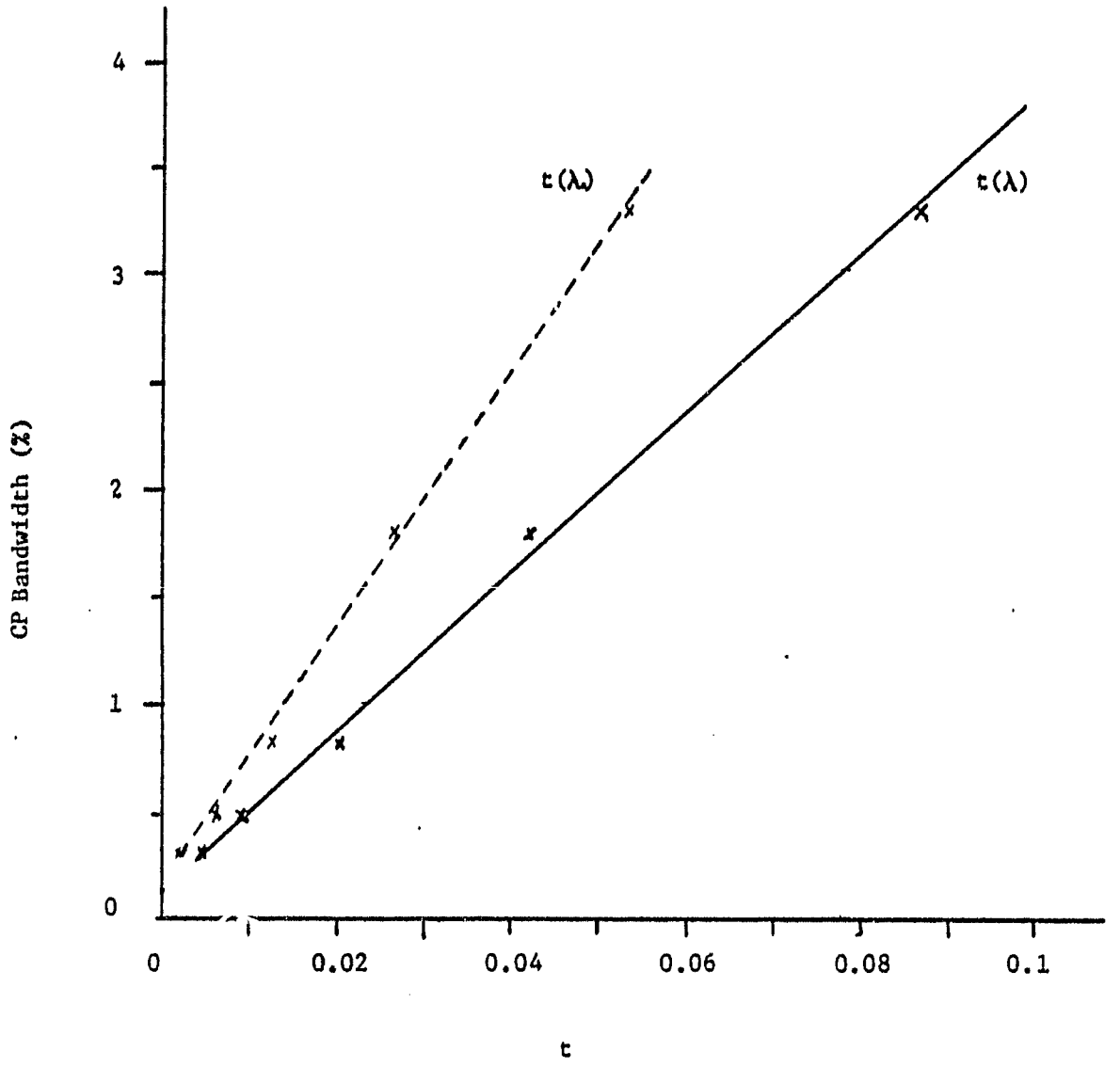

Figure 7. Bandwidth vs. the substrate thickness t, expressed in terms of free space wavelength, λ_o, or substrate dielectric wavelength λ.

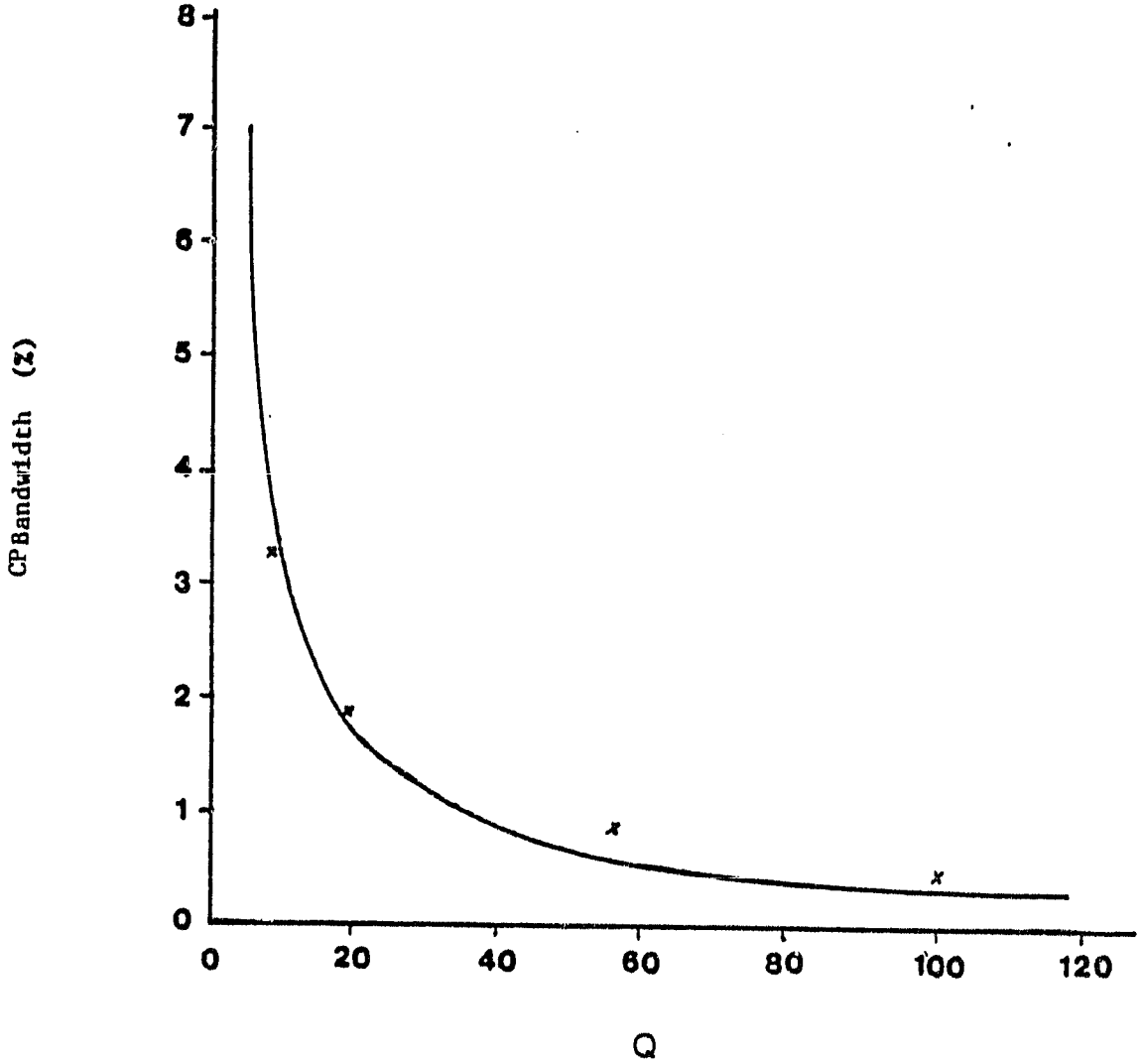

Figure 8. CP bandwidth vs. the quality factor Q.
——— Theory
xxx Experiment

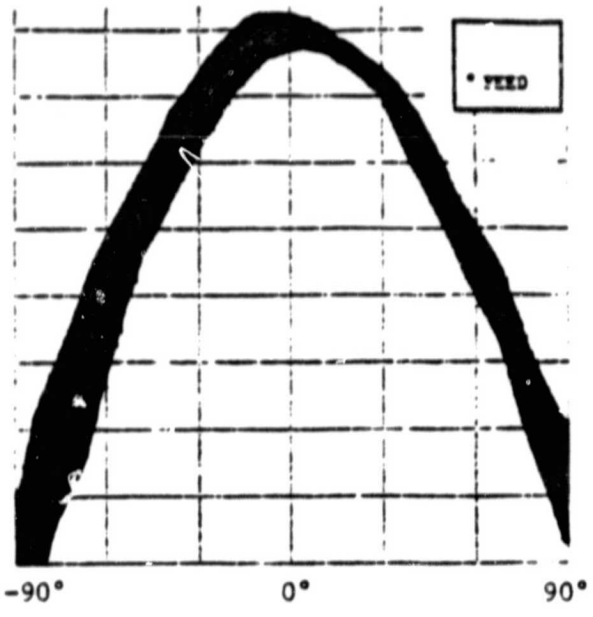

a) f=10.27 GHz

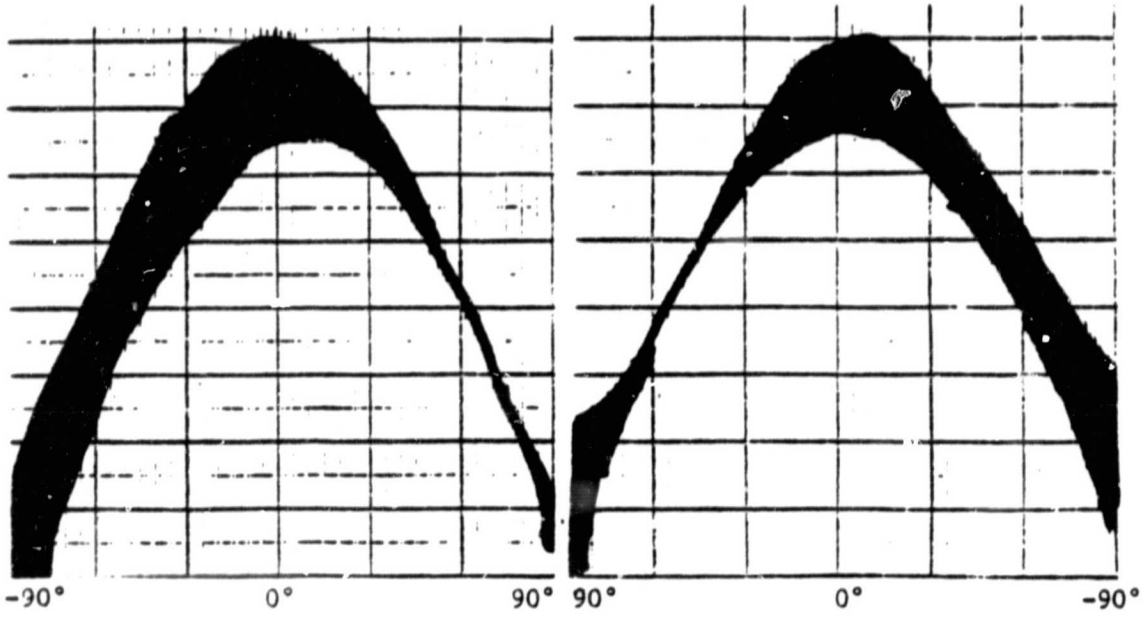

b) f=10.18 GHz

c) f=10.36 GHz

Figure 9. Field patterns of the microstrip antenna with dimension a = 1.088 cm, b = 0.90 cm, t = 0.08 cm, and feed point at x' = 0.2 cm, y' = 0.39 cm. All patterns were taken for ϕ = 0°.